Environ Monit Assess (2022) 194: 238
https://doi.org/10.1007/s10661-022-09763-6

Using multiple isotopes to identify sources and transport of nitrate in urban residential stormwater runoff

Qiyue Hu · Song Zhu · Zanfang Jin · Aijing Wu · Xiaoyu Chen · Feili Li

Received: 7 August 2021 / Accepted: 7 January 2022 / Published online: 2 March 2022

Abstract Increased nitrogen (N) from urban stormwater runoff aggravates the deterioration of aquatic ecosystems as urbanisation develops. The sources and transport of nitrate (NO_3^-) in urban stormwater runoff were investigated by analysing different forms of N, water isotopes ($\delta D\text{-}H_2O$ and $\delta^{18}O\text{-}H_2O$), and NO_3^- isotopes ($\delta^{15}N\text{-}NO_3^-$ and $\delta^{18}O\text{-}NO_3^-$) in urban stormwater runoff in a residential area in Hangzhou, China. The results showed that the concentrations of total N and nitrate N in road runoff were higher than those in roof runoff. Moreover, high concentrations of dissolved organic N and particulate N led to high total nitrogen (TN) concentrations in road runoff (mean: 3.76 mg/L). The high $\delta^{18}O\text{-}NO_3^-$ values (mean: $+60 \pm 13.1‰$) indicated that atmospheric deposition was the predominant NO_3^- source in roof runoff, as confirmed by the Bayesian isotope mixing model (SIAR model), contributing 84–98% to NO_3^-. Atmospheric deposition (34–92%) and chemical fertilisers (6.2–54%) were the main NO_3^- sources for the road runoff. The proportional contributions from soil and organic N were small in the road runoff and roof runoff. For the initial period, the NO_3^- contributions from atmospheric deposition and chemical fertilisers were higher and lower, respectively, than those in the middle and late periods in road runoff during storm events 3 and 4, while an opposite trend of road runoff in storm event 7 highlighted the influence of short antecedent dry weather period. Reducing impervious areas and more effective management of fertiliser application in urban green land areas were essential to minimize the presence of N in urban aquatic ecosystems.

Highlights
- High levels of DON, PN, and NO_3^- caused more TN in urban road runoff.
- Atmospheric deposition was the predominant NO_3^- source in urban roof runoff.
- Atmospheric deposition was 34–92%, and fertilisers were 6.2–53% for NO_3^- in urban road runoff.
- Soil and organic N had little contribution to NO_3^- both in roof and road runoff. NO_3^- from fertilisers was derived from green land in urban residential area.

Supplementary Information The online version contains supplementary material available at https://doi.org/10.1007/s10661-022-09763-6.

Q. Hu · Z. Jin (✉) · A. Wu · X. Chen · F. Li
College of Environment, Zhejiang University of Technology, Hangzhou 310032, China
e-mail: jinzanfang@zjut.edu.cn

S. Zhu
Zhejiang Construction Investment Environment Engineering Co., Ltd, Hangzhou 31000, China

Introduction

Increasing urbanisation worldwide has led to population explosion and changes in land use. Owing to the replacement of vegetation and permeable soil by impervious cover, a considerable amount of concrete floor constructed in urban areas causes stormwater

runoff to easily collect pollutants (Al Mamoon et al., 2019; Chong et al., 2012; Muller et al., 2020; Silva & da Silva, 2020). Urban stormwater runoff containing large quantities of contaminants, such as organic matter, phosphorus, and nitrogen, is considered to be an important pathway for the delivery of contaminants to urban aquatic ecosystems (Al Mamoon et al., 2019). Studies have investigated stormwater runoff pollution from impervious surfaces since the 1980s (Ballo et al., 2009; Chow & Yusop, 2014; Gromaire-Mertz et al., 1999; Kim et al., 2007; Myers et al., 1982; Yang & Toor, 2016). Yan et al. (2019) indicated that stormwater runoff was regarded as the largest source of total nitrogen, chemical oxygen demand (COD), and ammonium nitrogen (NH_4^+-N) in the Taihu Basin, China. Silva et al. (2019) demonstrated that increasing impervious areas in the catchment enhanced the nutrient inputs from stormwater runoff, carrying total suspended solids (TSS), total phosphorus, and nitrate (NO_3^-) into Lake Pampulha, Brazil, at the beginning of the wet season.

Nitrogen pollution loads account for a large proportion of pollution in urban stormwater and contribute to the degradation of urban water quality, especially owing to algal blooms and eutrophication (Carey et al., 2013; Yang et al., 2020). For example, it was reported that stormwater from impervious surfaces contributed 80% of dissolved N to urban rivers in Melbourne, Australia, contributing to the risk of water eutrophication (Taylor et al., 2005). Further, in recent years, eutrophication in urban aquatic ecosystems has hindered the sustainable development of cities in China (Li et al., 2019a). Therefore, it is important to identify N sources and to study their transport to minimise the transport of N by urban stormwater runoff to urban aquatic ecosystems.

Stable nitrogen and oxygen isotopes of NO_3^- (δ^{15}N-NO_3^- and δ^{18}O-NO_3^-) have been widely used to identify NO_3^- sources and reveal N transport and transformation in aquatic ecosystems due to an unique isotopic signature of each NO_3^- source (Chen et al., 2021; Liu et al., 2014, 2021; Ma et al., 2015; Margalef-Marti et al., 2021; Peng et al., 2012; Yuan et al., 2019; Yue et al., 2020). Generally, δ^{15}N-NO_3^- values range from 0.0‰ to + 25.0‰ for soil and organic N, -13.0‰ to + 13.0‰ for atmospheric deposition, -6.0‰ to + 6.0‰ for NH_4^+ fertiliser and NO_3^- fertiliser (Dong et al., 2021; Kendall et al., 2007; Xue et al., 2009). In recent years, with the development of technology, the nitrogen and oxygen isotopes combined with a Bayesian isotope mixing model (SIAR model) have been successfully applied to clarify the proportions of different N sources in surface water, groundwater, and surface runoff (Baral et al., 2018; Jani et al., 2020; Liu et al., 2021; Weitzman et al., 2021; Yang & Toor, 2016, 2017). Dong et al. (2021) investigated the values of δ^{15}N-NO_3^- and δ^{18}O-NO_3^- in a typical subtropical agricultural watershed and identified that nitrification of NH_4^+ mineralized from soil N and manure/sewage were the major sources of NO_3^- in stormwater runoff, accounting for 37–52% and 25–47% of the NO_3^- load, respectively. It was found that the δ^{15}N-NO_3^- values ranged from -11.5‰ to + 4.9‰ and that atmospheric deposition contributed 43–71% of NO_3^-, followed by chemical fertilisers (< 1–49%) in urban residential stormwater runoff in Florida (Yang & Toor, 2016). On the other hand, water isotopes (δD-H_2O and δ^{18}O-H_2O) can reveal the origin of water sources since different sources of water have distinct isotopic signatures (Rahal et al., 2021; Weitzman et al., 2021). Numerous studies have indicated that the combination of stable isotopes of NO_3^- with water isotopes can further enhance the ability to identify NO_3^- sources and its transformation processes in aquatic ecosystems (Gómez-Alday et al., 2022; Hu et al., 2019; Pastén-Zapata et al., 2014). For example, the δD-H_2O and δ^{18}O-H_2O values of river water, groundwater, and rainfall in the Yongan watershed of eastern China suggesting a substantial portion of river water may originate from groundwater and subsurface water sources, and the δ^{15}N-NO_3^- and δ^{18}O-NO_3^- values with SIAR model indicated that groundwater (43 ± 17%), soil N (33 ± 8%), and wastewater (25 ± 15%) were the dominant river NO_3^- sources (Hu et al., 2019).

In recent years, urban residential areas have been increasingly constructed due to the boom in the real estate industry in China, leading to an increase in impervious surfaces within residential areas, and accordingly, an increase in stormwater runoff carrying pollutants directly into urban rivers (Li et al., 2019b; Wen et al., 2019). Compared to China, more studies on stormwater runoff in residential areas have been conducted in other countries, whereas studies on stormwater runoff in China have focused more on non-point source pollution in agricultural areas (Sui et al., 2020). In residential areas, impervious surfaces

mainly comprise roads and roofs, and the different types of human activities on roads and roofs lead to the corresponding differences in characteristic pollutants (Yang & Toor, 2017). For instance, Kojima et al. (2011) demonstrated that N in road dust mainly originated from fertilisers and soil, while the N source in roof dust originated from atmospheric deposition.

In this study, stormwater runoff was collected from roads and roofs in an urban residential area, and the concentration of different forms of N and stable isotopes of NO_3^- ($\delta^{15}N\text{-}NO_3^-$ and $\delta^{18}O\text{-}NO_3^-$) were measured. The objectives were to evaluate the spatial and temporal distributions of the different forms of N and to quantify the major N sources in urban residential stormwater runoff. This study serves as a guideline for generating more effective mitigation strategies to reduce the concentration of N in urban aquatic ecosystems.

Materials and methods

Study site

The residential study area (30°17′N, 120°9′E) is located in Hangzhou, which is the political, economic, and cultural centre of Zhejiang Province, East China (Fig. 1). The continuously growing population in Hangzhou has increased from 8.89 million in 2014 to 10.36 million in 2019, and the urbanization rate of Hangzhou reached 78.5% in 2019 (HZSB, 2020). The residential area comprises approximately 12.7 ha, of which green land accounts for 27% and the rest are impervious surfaces (rooftops: 36%, driveways and sidewalks: 17%, and roads: 20%). The age of residential buildings in the study area is more than 30 years with 2525 households, and the area is served by a separate sewer system. We collected the roof runoff at the top of a five-storey residential building (approximately 15 m in height) which featured a flat and open-area cement roof without slope and any shelter. Rainwater on the roof is easily evacuated through the drainage ditch. Road runoff was collected on a residential road of bituminous concrete which featured tree, grass, and other plants planted on both sides of the roads. The overall study region is characterised by a subtropical monsoon climate with an annual average temperature of 15.7 ℃ and annual average rainfall of 1454 mm, of which 67% occurs during the wet season (March–September). The average annual rainfall was 1584.7 mm from 2019 to 2020, and monthly rainfall ranged from 37.7 to 374.7 mm in the wet season in Hangzhou (HZSB, 2020). The study period was from March to August in 2019 and 2020. And the urban runoff in this catcment finally enters into the Shangtang River, which is a tributary of the Grand Canal (Hangzhou).

Sampling and analysis

A weather application (Hangzhou weather network) showing the evolution of storm events was used to track storm events in the study area. Stormwater runoff samples were collected manually after identifying a major storm event. An acid-washed polyethylene container was used to gather runoff samples before the runoff flowed into the rain drainage systems. The roof and road runoff were collected at the top of the five-storey residential building (Site A) and on the road in the residential area (Site B), respectively

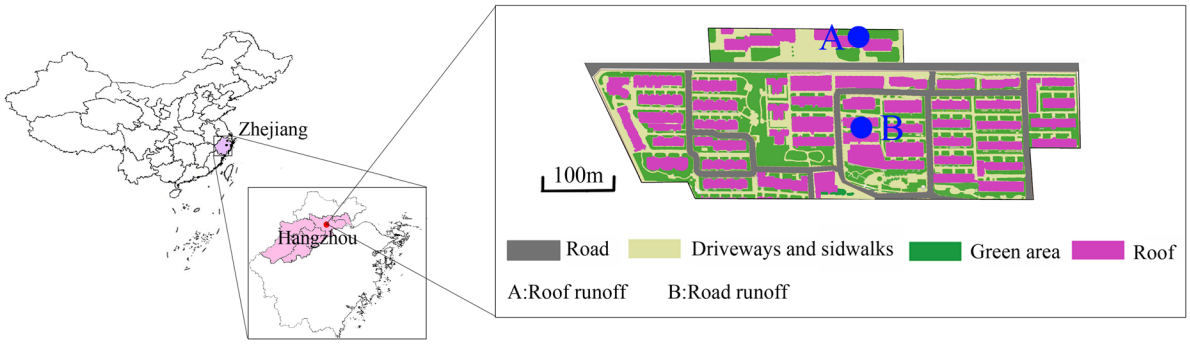

Fig. 1 Sampling sites in the study area

Table 1 Information on runoff sampling in an urban residential area from 2019 to 2020

Storm event	1	2	3	4	5	6	7
Date	March 27, 2019	May 13, 2019	June 25, 2019	August 09, 2019	May 15, 2020	June 16, 2020	August 28, 2020
Antecedent dry weather period (d)	12	13	8	6	4	4	1
Rainfall intensity during sampling period (mm/h)	4.65	2.27	4.65	9.55	3.2	8.17	4
The rainfall amount during sampling period (mm)	9.3	3.4	9.3	19.1	6.4	16.3	8

(Table 1). At each catchment site, samples were collected at 5 min intervals within 1.5–2 h during each storm and were placed in a 500 mL plastic bottle. The stormwater runoff samples were collected during seven storm events, leading to a total of 321 samples (165 roof and 156 road runoff samples) (Fig. 1). After sampling, a portion of the samples was filtered through 0.45 μm membrane filters (Whatman) into 100 mL acid-washed polyethylene bottles on the sampling day and stored in a refrigerator at -20 ℃ until the analysis of dissolved total nitrogen (DTN), major ions (NH_4^+, NO_2^- and NO_3^-), and isotopes. The other portion was not filtered and stored at -4 ℃ for TN and COD analysis within 48 h.

TN and DTN were measured using the alkaline potassium persulfate digestion ultraviolet spectrophotometric method (HJ636-2012). Total suspended solids (TSS) and COD were analysed using the gravimetric method (GB11901-89) and the fast digestion-spectrophotometric method (HJ/T399-2007), respectively. The concentrations of NH_4^+, NO_2^-, and NO_3^- were measured using ion chromatography (Dionex ICS-900), and the detection limits of NH_4^+, NO_2^-, and NO_3^- were 0.03, 0.02, and 0.02 mg/L, respectively. Additionally, replicates were used for the determination of each sample, including TN, DTN, NH_4^+, NO_2^-, and NO_3^-, TSS, COD, δD-H_2O, δ^{18}O-H_2O, δ^{15}N-NO_3^- and δ^{18}O-NO_3^-. The NO_2^- concentrations in most of the samples were below the detection limit (BDL); therefore, dissolved inorganic nitrogen (DIN) was defined as the sum of NH_4^+-N and nitrate nitrogen (NO_3^--N). The dissolved organic nitrogen (DON) and particulate nitrogen (PN) were calculated using the following mass balance: [DON] = [DTN]—[DIN] and [PN] = [TN]—[DTN].

Twenty-two road runoff samples were analysed for hydrogen and oxygen isotopes of water (δD-H_2O and δ^{18}O-H_2O) using an isotopic water analyser (Picarro L2140-i). The precisions of δD-H_2O and δ^{18}O-H_2O were ± 0.5‰ and ± 0.1‰, respectively. Thirty-two roof runoff and thirty-five surface runoff samples were analysed for stable nitrogen and oxygen isotopes of NO_3^- (δ^{15}N-NO_3^- and δ^{18}O-NO_3^-) which were measured following the bacterial denitrification method (Kaiser et al., 2007; McIlvin & Casciotti, 2011). Nitrite (NO_2^-) in the samples was reduced to nitric oxide (NO) using ascorbic acid (pH < 3.5), and then, the NO produced was continually degassed with an inert gas (helium) during the reaction. In brief, denitrifying bacteria (*Pseudomonas aureofaciens*) lacking gaseous nitrous oxide (N_2O), converted NO_3^- from the water samples to N_2O through reductase activity. Then, the N_2O was stripped by helium carrier gas and thermally decomposed to N_2 and O_2. The isotopic ratios of N_2 (^{15} N/^{14} N) and O_2 (^{18}O/^{16}O) were measured by a mass spectrometer (Thermo Delta V Advantage). The analytical errors for δ^{15}N-NO_3^- and δ^{18}O-NO_3^- were ± 0.3‰ and ± 0.5‰, respectively. In this paper, isotopic results are expressed as δ values (per mil unit), such that

$$\delta(^0/_{00}) = 1000 \times \left(\frac{R_{sample}}{R_{standard}} - 1 \right),$$

where R is the isotopic ratios (^{15} N/^{14} N, ^{18}O/^{16}O, and D/H). The standard of ^{15} N/^{14} N was atmospheric air

(AIR), and the collective standard of $^{18}O/^{16}O$ and D/H was the Vienna Standard Mean Ocean Water (VSMOW).

SIAR model

The proportions of the different NO_3^- source contributions were evaluated by the SIAR model. The SIAR model can be expressed as follows (Parnell et al., 2010):

$$X_{ij} = \sum_{k=1}^{K} p_k\left(S_{jk} + C_{jk}\right) + \varepsilon_{ij};$$

$$S_{ij} \sim N\left(\mu_{jk}, \omega_{jk}^2\right);$$

$$C_{ij} \sim N\left(\lambda_{jk}, \tau_{jk}^2\right);$$

$$\varepsilon_{ij} \sim N\left(0, \sigma_j^2\right);$$

where X_{ij} is the isotope value j of the mixture i ($i=1$, 2, 3,…, N, and $j=1$, 2, 3,…, J); S_{jk} is the isotope value j in source k ($k=1$, 2, 3,…, K), which conforms to a normal distribution with a mean of μ_{jk} and a standard variance of ω_{jk}^2; C_{jk} is the fractionation coefficient for isotope j for source k, which is a standard distribution with a mean value of λ_{jk} and a variance of τ_{jk}^2; and ε_{ij} is the residual error, which is used to characterise the remaining unquantified variation between the individual mixed samples and is a normal distribution with a mean value of 0 and a variance of σ_j^2. The variable p_k is the proportional contribution of source k, estimated using the SIAR model.

Results and discussion

N concentration and N forms in stormwater runoff

The concentrations of TN, DTN, NH_4^+-N, NO_3^--N, PN and DON in roof runoff and road runoff for 2019–2020 are shown in Table 2. The concentrations of TN, NH_4^+-N, and NO_3^--N in the roof runoff of seven storm events ranged from 0.26–6.13 (mean 1.23 mg/L), 0.03–1.96 (mean 0.42 mg/L), BDL–1.69 (mean 0.26 mg/L), respectively. The concentrations of TN, NH_4^+-N, and NO_3^--N in the road runoff of the same seven storm events were higher than those in the roof runoff (TN: 0.65–12.7 (mean 3.76 mg/L), NH_4^+-N: BDL–5.28 (mean 0.50 mg/L), and NO_3^--N: BDL–3.05 (mean 0.50 mg/L)). The concentrations of PN and DON in roof and road runoff also showed the same trend as those of TN, NH_4^+-N, and NO_3^--N. In addition, the concentrations of TN, PN, and DON in road runoff were more than three times higher than as those in the roof runoff in the same storm event, proving the important influence of surrounding land use on N in stormwater runoff (Table 2). Road runoff is an important source of nonpoint pollution in urban aquatic ecosystems because the N compounds within the road dust, chemical fertiliser, soil materials, pet waste, and leaf litter on road surfaces are eventually washed into stormwater runoff (Janke et al., 2017; Lusk & Toor, 2016; Yang & Toor, 2017). In contrast, human activities had relatively little impact on the roof runoff, while atmospheric deposition and organic N, such as bird and rodent droppings, were the main N sources on the cement roof surfaces (Song et al., 2019). Moreover, the TN concentration was dominated by PN and DON in road runoff, while NH_4^+-N and NO_3^--N were the major N compounds in roof runoff (Table 2). The results were consistent with those of Vaze and Chiew (2004), who found that the proportion of DTN in TN ranged between 20 and 50%, and proportion of PN in TN ranged from 50 to 80% in road runoff in Australia. It was suggested that roads were more likely to accumulate particulate matter than roofs, and that the particulate matter in the soil on the sides of the roads was easily mobilised and transported to the impervious surface through stormwater runoff. Previous studies have also documented that climatic parameters such as the frequency and intensity of storms and antecedent rainfall conditions have significant impacts on the concentrations of N in stormwater runoff, leading to a wide range of N concentrations in stormwater runoff (Yang & Lusk, 2018). The event mean concentration of TN average value in road runoff in this study (3.61 mg/L) was higher than that in road runoff in humid subtropical urban residential areas in Tampa, Florida, (TN: 0.42 mg/L) and much lower than that in a study conducted on road runoff in a semi-arid urban residential area in the Aliso Creek watershed, California (TN: 10.85 mg/L) (Toor et al., 2017; Yang & Toor, 2017).

Significantly positive correlations ($P<0.01$) were found between antecedent dry weather period and

Table 2 Statistical parameters of different N forms, TSS, COD, and the NO_3^--N/NH_4^+-N ratios in roof runoff and road runoff in an urban residential area from 2019 to 2020

		TN	DTN	NH_4^+-N	NO_3^--N	DIN	PN	DON	TSS	COD	NO_3^--N/NH_4^+-N
		mg/L	mg/L	mg/L	mg/L	mg/L	mg/L	mg/L	mg/L	mg/L	
roof runoff											
Storm event 1	mean	1.35	1.12	0.55	0.29	0.84	0.23	0.28	66.2	12.3	0.49
n = 22	min	0.39	0.25	0.07	0.03	0.09	0.04	0.03	6	5.19	0.28
	max	3.54	3.05	1.65	1.12	2.77	0.53	0.86	114	30.4	0.85
Storm event 2	mean	2.63	2.42	0.86	0.57	1.43	0.20	0.99	45	23.7	0.61
n = 23	min	0.68	0.66	0.16	0.07	0.24	0.01	0.24	2	5.56	0.22
	max	6.13	5.92	1.96	1.69	3.25	0.72	2.67	94	53.6	1.85
Storm event 3	mean	0.61	0.55	0.16	0.12	0.28	0.06	0.28	31.3	12.7	0.51
n = 24	min	0.26	0.20	0.09	0.02	0.11	0.01	0.04	5	4.6	0.23
	max	2.81	2.46	0.63	1.14	1.77	0.35	0.73	92	38.6	1.81
Storm event 4	mean	0.60	0.49	0.19	0.06	0.25	0.10	0.24	47	16.1	0.29
n = 24	min	0.31	0.25	0.07	BDL	0.08	0.01	0.06	12	5.61	0.00
	max	1.59	1.56	0.60	0.26	0.86	0.30	0.70	112	51.7	0.81
Storm event 5	mean	0.92	0.70	0.16	0.13	0.29	0.22	0.41	28.9	31.8	0.97
n = 24	min	0.48	0.40	0.03	0.03	0.08	0.03	0.18	0	11.2	0.33
	max	1.83	1.77	0.64	0.46	1.10	0.63	0.79	78	68.1	1.91
Storm event 6	mean	1.48	1.26	0.56	0.36	0.92	0.22	0.35	33.1	24.6	0.66
n = 25	min	0.33	0.21	0.13	0.08	0.21	0.01	0.00	2	5.38	0.43
	max	3.99	3.87	1.76	1.07	2.83	0.61	1.04	138	62.3	1.05
Storm event 7	mean	1.06	0.98	0.45	0.30	0.74	0.08	0.24	12.6	8.21	0.69
n = 23	min	0.71	0.65	0.33	0.08	0.43	0.02	0.01	2	2.69	0.22
	max	1.56	1.46	0.72	0.47	1.19	0.17	0.59	46	18.9	1.16
road runoff											
Storm event 1	mean	3.78	1.90	0.41	0.76	1.17	1.88	0.74	142	78.2	2.04
n = 25	min	0.74	0.13	0.04	BDL	0.04	0.47	0.04	8	274	0.00
	max	7.21	5.69	1.41	3.05	4.46	4.70	2.30	508	192.6	5.87
Storm event 2	mean	6.82	4.08	1.12	0.26	1.37	2.73	2.71	262.6	264.8	0.58
n = 20	min	1.02	0.74	BDL	0.01	0.02	0.21	0.61	80	86.3	0.01
	max	12.70	9.69	5.28	1.64	6.04	4.81	6.56	544	412.2	3.47
Storm event 3	mean	3.87	3.12	0.71	0.95	1.66	0.76	1.46	188.8	168	1.45
n = 24	min	1.99	1.68	0.28	0.41	0.88	0.04	0.25	74	52.4	0.66
	max	8.78	7.24	1.98	2.41	4.39	1.55	4.67	576	439.8	2.45
Storm event 4	mean	2.39	1.35	0.17	0.28	0.46	1.04	0.90	223	100.8	2.22
n = 24	min	1.45	0.29	BDL	BDL	0.01	0.15	0.04	48	37.4	NC
	max	5.09	3.75	0.87	0.60	1.45	3.48	2.30	462	242	6.70
Storm event 5	mean	4.79	1.67	0.38	0.12	0.50	3.13	1.16	383.3	266.9	0.37
n = 20	min	2.18	0.63	BDL	BDL	BDL	0.83	0.27	52	96.9	NC
	max	10.21	5.28	0.94	0.31	0.96	6.81	4.32	978	431.5	1.12
Storm event 6	mean	2.07	1.37	0.48	0.29	0.77	0.70	0.60	198.4	86.1	1.60
n = 20	min	0.65	0.40	0.01	BDL	0.15	0.21	0.25	80	34.7	0.00
	max	4.48	3.47	1.54	1.22	2.77	2.13	1.50	484	217.8	9.15
Storm event 7	mean	2.95	1.67	0.34	0.66	1.00	1.28	0.67	138	83.7	2.33
n = 23	min	1.10	0.71	0.11	0.21	0.32	0.04	0.39	4	8.08	0.75

Table 2 (continued)

	TN	DTN	NH_4^+-N	NO_3^--N	DIN	PN	DON	TSS	COD	NO_3^--N/NH_4^+-N
	mg/L	mg/L	mg/L	mg/L	mg/L	mg/L	mg/L	mg/L	mg/L	
max	6.61	2.82	0.66	1.48	2.08	3.94	1.10	444	253.5	4.00

n: Number of the samples

BDL: below the detection limit;

NC: When the NH_4^+-N concentrations were below the detection limit, the NO_3^--N/NH_4^+-N ratios were not calculated

TN, DTN, NH_4^+-N, and DON concentrations, both in roof runoff and road runoff, revealing that N concentrations in stormwater runoff are linked to the duration of dry periods before storm events (Table S1). Lewis and Grimm (2007) also reported high NH_4^+-N concentration in stormwater runoff in arid urban catchments after a longer antecedent dry period. Higher concentrations of TN, DTN, NH_4^+-N, and DON were observed in roof and road runoff during storm event 2, as compared to those in other storm events. This is attributed to the longer antecedent dry weather period (13 days) preceding 13 May 2019. As pollutants accumulate on impervious surfaces during antecedent dry periods, the stormwater runoff after a longer antecedent dry weather period carries more pollutants (Lewis & Grimm, 2007; Li et al., 2007a; Zhi et al., 2018). The PN and DON concentrations in the road runoff were higher in May than those in the other months (Table 2). Furthermore, higher concentrations of PN corresponded to the higher concentrations of TSS in road runoff (Table 2). Similarly, higher concentrations of DON were consistent with the higher concentrations of COD in road runoff (Table 2). Significantly positive correlations ($P < 0.01$) were found between TSS and PN, COD, and DON concentrations, in road runoff (Table S1). This may be attributed to extensive plant growth during May, which is a warm and humid month in late spring. During this time, organic matter, including leaf litter, flower debris, pollen, and seeds, is expected to reach the ground and eventually enter into stormwater runoff, increasing the organic N load of the road runoff in the urban residential area. These results are in agreement with Janke et al. (2017), who found that seasonal peaks of N in urban stormwater runoff coincided with spring leaf-out and flowering.

The mean concentrations of NO_3^--N were lower than the mean concentrations of NH_4^+-N in roof runoff, while the opposite was true for in road runoff (Table 2). NO_3^--N concentrations in rainwater of Hangzhou were lower than NH_4^+-N concentrations, and the mean NO_3^--N/NH_4^+-N ratio was found to be 0.87 from 2015 to 2017 (Jin et al., 2019). In this study, all mean NO_3^--N/NH_4^+-N ratios in the roof runoff of the seven storm events were lower than 1.0, indicating that atmospheric deposition was the dominant N source in the roof runoff. The NO_3^--N/NH_4^+-N ratios in road runoff varied widely (0.37–2.33). In addition to atmospheric deposition, it was found that anthropogenic inputs, such as chemical fertilisers, soil materials, pet waste, and leaf litter, also influenced the NO_3^--N and NH_4^+-N concentrations in road runoff. NO_3^--N may have been preferentially washed out from surface deposits, and NH_4^+-N could have been easily absorbed by surface deposits (Kojima et al., 2011; Wang et al., 2019). However, the NO_3^--N/NH_4^+-N ratios in road runoff in May (storm events 2 and 5) were much lower than those in other months (Table 2). On the one hand, due to the increased air temperature and humidity in May, the activities of microbes were likely enhanced; therefore, the mineralisation of tree branches, leaf litter, flower debris, and soil organic N was likely a significant contributor to the NH_4^+-N in road runoff. On the other hand, low rainfall in May would not have been conducive to NO_3^--N export in stormwater runoff (Kaushal et al., 2014). The above two reasons could explain why the NO_3^--N concentrations were lower and the NH_4^+-N concentrations were higher in road runoff in May than in other months.

The temporal variation of N forms in roof and road runoff during the seven storm events is shown in Fig. S1. The concentrations of TN, NH_4^+-N, and NO_3^--N in roof and road runoff were higher in the beginning of the storm event and then gradually stabilized with an increase in rainfall duration. Climate variables such as the frequency and intensity of storms are important factors that influence N transport in stormwater runoff, and NO_3^--N exports in stormwater

runoff increased during strong storms (Kaushal et al., 2014; Li et al., 2015). For example, the comprehensive wind and rain intensity index of Super Typhoon Lekima was 158.6, and the rainfall amount during the sampling period was 19.1 mm on 9 August 2019 (NMC, 2019). The onrush of water that accompanied strong winds during Super Typhoon Lekima caused a strong scouring effect on the land. As a result, the temporal variations in NO_3^--N concentrations in the road runoff of storm event 4 (9 August 2019) showed significant fluctuations. Owing to the low rainfall, the temporal variations of NO_3^--N concentrations in road runoff during storm events 2 and 5 were maintained at a low level. The antecedent conditions could have also affected N transport in the stormwater runoff (Lee et al., 2002; Taebi & Droste, 2004). Thus, it is considered that the temporal variations of TN, NO_3^--N, and NH_4^+-N concentrations in the roof runoff of event 7 were more stable owing to a lower rainfall amount and relatively short antecedent dry weather period.

Water sources of stormwater runoff

Unlike roof runoff, road runoff can originate from a combination of various water sources, such as rainfall and the overflow of sewer system in urban residential areas. Therefore, water isotopes were used to identify the water sources in the road runoff. The values of $\delta D\text{-}H_2O$ ranged from -44.3‰ to -26.1‰ (mean -34.7 ± 7.6‰), and the $\delta^{18}O\text{-}H_2O$ values ranged from -6.5‰ to -4.3‰ (mean -5.4 ± 0.9‰) in road runoff in storm events 3 (n = 11) (Fig. 2 and Table 3). The values of $\delta D\text{-}H_2O$ ranged from -72.2‰ to -67.8‰ (mean -70.4 ± 1.4‰), and the $\delta^{18}O\text{-}H_2O$ values ranged from -10.5‰ to -9.6‰ (mean -10.1 ± 0.3‰) in road runoff in storm events 7 (n = 11) (Fig. 2 and Table 3). The relationship between $\delta^{18}O\text{-}H_2O$ and $\delta D\text{-}H_2O$ in road runoff could be described as $\delta D\text{-}H_2O = 7.6\ \delta^{18}O\text{-}H_2O + 6.2$ ($R^2 = 0.99$), which was remarkably close to the local meteoric water line (LMWL: $\delta D\text{-}H_2O = 8.4\ \delta^{18}O\text{-}H_2O + 17.5$) and the global meteoric water line (GMWL: $\delta D\text{-}H_2O = 8.0\ \delta^{18}O\text{-}H_2O + 10.0$) (Jin et al., 2021a; Craig, 1961). It was suggested that water in the road runoff mainly originated from local rainwater in the study area. The slope and intercept of this isotopic line for the road runoff samples were lower than those of the LMWL and GMWL, implying that slight evaporation occurred during runoff generation. Owing to the high temperature during the study period and the impervious surface in the study area (73%), evaporation was likely to take place as runoff travelled over the impervious surface. (see Tables 4 and 5)

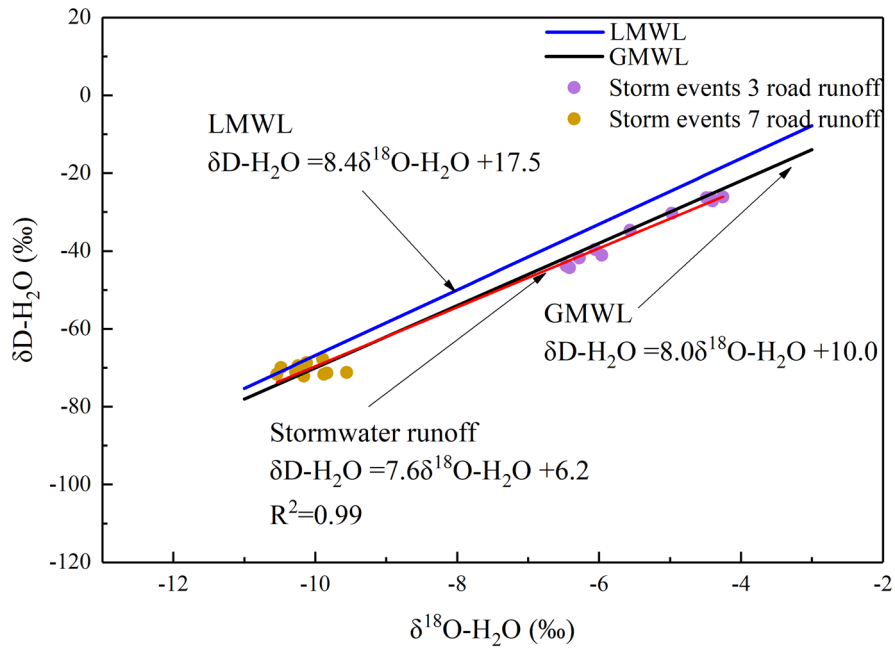

Fig. 2 Relationship between $\delta^{18}O\text{-}H_2O$ and $\delta D\text{-}H_2O$ for road runoff (n = 22)

Table 3 The $\delta^{15}N\text{-}NO_3^-$ and $\delta^{18}O\text{-}NO_3^-$ values and the $\delta D\text{-}H_2O$ and $\delta^{18}O\text{-}H_2O$ values in the roof runoff and road runoff and the $\delta^{15}N\text{-}NO_3^-$ and $\delta^{18}O\text{-}NO_3^-$ values of NO_3^- sources used in SIAR

Sample		$\delta^{15}N\text{-}NO_3^-$		$\delta^{18}O\text{-}NO_3^-$		$\delta D\text{-}H_2O$		$\delta^{18}O\text{-}H_2O$	
		Mean	SD	Mean	SD	Mean	SD	Mean	SD
Roof runoff	Storm event 3 (n = 10)	-1.41	1.19	+57.53	6.26				
	Storm event 4 (n = 11)	-2.45	1.43	+46.47	3.53				
	Storm event 7 (n = 11)	-7.84	2.02	+75.66	2.36				
Road runoff	Storm event 3 (n = 13)	-2.95	2.41	+31.17	10.11	-34.67	+7.62	-5.39	0.89
	Storm event 4 (n = 11)	-2.17	4.52	+22.20	5.79				
	Storm event 7 (n = 11)	-3.73	2.45	+70.01	2.66	-70.43	+1.41	-10.11	0.29
	Atmospheric deposition [a]	-1.00	1.90	+60.20	12.50				
	NH_4^+ Fertiliser [b]	-0.20	2.28	-2.00	8.00				
	NO_3^- Fertiliser [c]	+1.10	2.78	+21.30	3.01				
	Soil and organic N [d]	+7.50	5.23	-2.00	8.00				

n: Number of the samples

[a]Jin et al., 2019; [b]Curt et al., 2004; Kendall et al., 2007; Li et al., 2007a; Li et al., 2007b; Yang & Toor, 2016; [c]Curt et al., 2004; Kendall et al., 2007; Yang & Toor, 2016; [d]Bedard-Haughn et al., 2003; Curt et al., 2004; Divers et al., 2014; Kendall et al., 2007;Yang & Toor, 2016

NO_3^- sources in stormwater runoff

Identifying NO_3^- sources and NO_3^- transport in stormwater runoff

The $\delta^{18}O\text{-}NO_3^-$ values in roof runoff varied from +49.1‰ to +68.6‰ (mean: +57.5 ± 6.3‰) in storm events 3 (n = 10), from +39.9‰ to +53.1‰ (mean: +46.5 ± 3.5‰) in storm events 4 (n = 11), and from +72.3‰ to +79.8‰ (mean: +75.7 ± 2.4‰) in storm events 7 (n = 11) (Fig. 3 and Table 3). The $\delta^{18}O\text{-}NO_3^-$ values in road runoff varied from +21.9‰ to +50.2‰ (mean: +31.2 ± 10.1‰) in storm events 3 (n = 13), from +15.6‰ to +36.6‰ (mean: +22.2 ± 5.8‰) in storm events 4 (n = 11), and from +65.4‰ to +74.3‰ (mean: +70.0 ± 2.7‰) in storm events 7 (n = 11) (Fig. 3 and Table 3). Temporal variations of $\delta^{18}O\text{-}NO_3^-$ in stormwater runoff during storm events 3, 4, and 7 are shown in Fig. 4. The temporal variations of $\delta^{18}O\text{-}NO_3^-$ in roof runoff were limited, and the $\delta^{18}O\text{-}NO_3^-$ values in the roof runoff were higher than those in road runoff. In general, $\delta^{18}O\text{-}NO_3^-$ values range from +25.0‰ to +75.0‰ for atmospheric deposition, +17.0‰ to +25.0‰ for NO_3^- fertilisers, -5.0‰ to +15.0‰ for NO_3^- derived from nitrification (Kendall et al., 2007; Xue et al., 2009; Yue et al., 2020). The $\delta^{18}O\text{-}NO_3^-$ values of rainwater and dry deposition in Hangzhou in wet season were +31.5–+71.6‰ (mean: +57.4‰), and +24.5–+79.2‰ (mean: +62.5‰), respectively (Jin et al., 2021b; Jin et al., 2019). The high $\delta^{18}O\text{-}NO_3^-$ values in roof runoff were in the range of $\delta^{18}O\text{-}NO_3^-$ values of global atmospheric deposition and similar to the $\delta^{18}O\text{-}NO_3^-$ values of rainwater and dry deposition in Hangzhou, implying that the atmospheric deposition (both dry and wet) was the dominant NO_3^--N source in roof runoff (Fig. 3). The higher values of $\delta^{18}O\text{-}NO_3^-$ in roof and road runoff for storm event 7 than those in other events resulted from the influence of the high $\delta^{18}O\text{-}NO_3^-$ values of atmospheric deposition (Fig. 4). The $\delta^{18}O\text{-}NO_3^-$ values in road runoff were lower than those in roof runoff and were further from the $\delta^{18}O\text{-}NO_3^-$ values in rainwater and dry deposits in Hangzhou, indicating that NO_3^--N from other sources was carried with the urban stormwater runoff.

The $\delta^{15}N\text{-}NO_3^-$ values ranged from -10.7‰ to +1.4‰ (mean: -4.0 ± 3.3‰) in roof runoff, and from -8.6‰ to +8.4‰ (mean: -2.9 ± 3.1‰) in road runoff (Fig. 3 and Table 3). The $\delta^{15}N\text{-}NO_3^-$ values of rainwater (-4.4‰ to +3.6‰) and dry deposition (-1.0‰ to +5.8‰) in Hangzhou during the wet season were in the range of the $\delta^{15}N\text{-}NO_3^-$ values in road runoff, suggesting that other NO_3^- sources contributed to road runoff in addition to the atmospheric NO_3^- (Fig. 3) (Jin et al., 2021b; Jin

Table 4 The concentrations of N, TSS, COD, Major ions (NH_4^+, NO_2^-, NO_3^-) in individual 7 stormwater runoff events

Storm event	Site	Number of samples	Time	Rainfall amount	TN	DTN	TSS	COD	NH_4^+	NO_3^-
			(min)	(mm)	(mg/L)					
20,190,327	A	22	0	1.48	3.54	3.05	114	28.15	2.12	4.96
Storm event 1			5	0.74	2.67	2.36	104	30.37	1.66	3.50
			10	0.37	2.90	2.48	84	25.93	1.74	2.80
			15	0.74	2.10	1.80	72	9.63	1.17	2.12
			20	0.15	2.15	1.90	12	6.30	1.10	2.56
			25	0.37	1.84	1.80	34	6.30	1.06	1.19
			30	0.37	1.43	1.37	102	14.81	0.79	1.53
			35	0.15	1.89	1.68	96	10.00	0.72	1.12
			40	0.74	1.32	1.26	88	13.33	0.86	1.63
			45	0.74	0.96	0.76	78	19.63	0.59	0.95
			50	1.11	0.55	0.51	86	5.93	0.32	0.41
			55	0.37	0.52	0.39	96	11.11	0.23	0.44
			60	0.52	0.39	0.29	64	11.85	0.09	0.15
			65	0.30	0.39	0.26	100	10.74	0.08	0.12
			70	0.37	0.48	0.25	18	5.56	0.17	0.24
			75	0.37	0.48	0.32	92	5.19	0.19	0.29
			80	0.15	0.50	0.29	6	9.63	0.20	0.32
			85	0.07	0.83	0.49	72	10.00	0.18	0.19
			90	0.07	0.89	0.78	76	7.78	0.27	0.78
			95	0.04	0.85	0.31	40	7.78	0.28	0.27
			100	0.04	1.36	1.06	14	8.52	0.79	1.27
			105	0.04	1.63	1.27	8	12.96	0.97	1.56
	B	25	0	1.48	7.07	5.68	108	83.33	1.81	13.53
			5	0.74	7.21	5.69	204	75.19	1.57	9.63
			10	0.37	6.85	2.15	356	192.59	0.55	3.98
			15	0.74	6.71	2.84	508	185.19	0.78	2.72
			20	0.15	5.46	0.99	148	160.37	0.29	0.61
			25	0.37	6.06	3.88	148	84.07	1.23	7.82
			30	0.37	4.12	2.61	40	74.07	0.84	5.30
			35	0.15	5.18	1.89	376	89.26	0.65	1.84
			40	0.74	3.87	1.32	92	40.74	0.56	3.01
			45	0.74	4.38	3.16	168	53.33	0.87	5.00
			50	1.11	2.85	1.93	68	34.07	0.48	1.12
			55	0.37	1.22	0.39	96	62.96	0.06	0.80
			60	0.52	3.22	1.99	160	41.85	0.57	4.28
			65	0.30	4.11	0.90	264	121.48	0.15	1.12
			70	0.37	2.25	1.55	176	97.41	0.45	3.43
			75	0.37	1.88	1.15	164	45.56	0.21	0.51
			80	0.15	3.15	1.44	48	81.48	0.44	2.85
			85	0.07	3.35	1.44	120	39.63	0.09	0.17
			90	0.07	1.09	0.13	20	41.11	0.05	/
			95	0.04	2.22	1.47	8	47.78	0.16	3.17
			100	0.04	0.74	0.28	18	27.04	0.10	0.39
			105	0.04	2.44	0.62	12	60.74	0.14	2.13

Table 4 (continued)

Storm event	Site	Number of samples	Time (min)	Rainfall amount (mm)	TN (mg/L)	DTN	TSS	COD	NH_4^+	NO_3^-
			110	0.04	3.45	1.41	92	57.41	0.52	3.81
			115	0.04	2.66	1.19	68	69.26	0.21	3.49
			120	0.03	2.97	1.47	88	88.15	0.33	3.25
20,190,513	A	23	0	0.22	6.13	5.92	68	53.62	2.00	7.50
Storm event 2			5	0.16	4.64	3.92	72	37.85	1.83	4.73
			10	0.11	3.59	3.48	66	35.54	1.69	3.76
			15	0.11	4.15	3.56	62	22.08	1.44	3.48
			20	0.05	3.31	3.22	74	32.85	0.99	1.99
			25	0.11	3.47	3.37	88	19.38	1.31	3.30
			30	0.27	3.69	3.27	86	24.00	1.88	3.26
			35	0.03	3.42	3.28	54	18.62	1.17	1.83
			40	0.03	3.83	3.52	32	23.62	2.05	3.94
			45	0.05	3.51	3.32	94	19.77	2.53	4.70
			50	0.03	3.86	3.66	76	24.00	2.32	5.26
			55	0.05	3.10	2.79	20	18.23	0.87	5.52
			60	0.22	2.13	2.12	42	16.69	1.38	2.85
			65	0.54	1.19	1.01	40	11.85	0.40	0.46
			70	0.43	1.69	1.43	12	5.56	0.31	0.47
			75	0.27	1.80	1.59	8	19.26	0.68	1.30
			80	0.27	1.81	1.72	22	10.00	0.70	0.77
			85	0.32	0.75	0.72	26	28.89	0.24	0.49
			90	0.03	0.68	0.66	2	13.70	0.32	0.57
			95	0.03	1.22	0.80	58	51.48	0.60	0.45
			100	0.03	0.77	0.75	4	32.59	0.21	0.36
			105	0.03	0.81	0.77	6	9.63	0.34	0.32
			110	0.02	0.95	0.89	22	14.81	0.27	0.48
	B	20	0	0.22	12.70	9.69	544	412.22	6.79	3.36
			5	0.16	11.77	8.47	414	318.15	2.51	3.42
			10	0.11	10.33	7.30	262	278.52	5.35	0.12
			15	0.11	10.90	7.35	362	337.78	0.80	0.77
			20	0.05	11.04	7.48	220	297.41	4.23	1.98
			25	0.11	10.12	6.18	338	346.67	0.97	7.25
			30	0.27	9.81	5.00	474	244.81	1.59	2.00
			35	0.03	8.89	4.31	312	242.22	0.93	1.09
			40	0.03	7.25	4.85	276	218.15	1.59	0.85
			45	0.05	5.87	3.50	368	277.78	0.86	0.37
			50	0.03	8.63	4.78	384	258.15	1.33	0.05
			55	0.05	6.80	2.59	248	210.00	0.94	0.04
			60	0.22	5.31	2.10	106	399.63	0.08	0.13
			65	0.54	1.98	0.92	80	152.59	/	0.12
			70	0.43	3.03	0.74	106	390.00	/	0.09
			75	0.27	3.78	0.89	310	307.04	0.03	0.08
			80	0.27	2.13	0.75	92	120.37	0.04	0.47
			85	0.32	3.45	2.96	100	190.00	0.53	0.33

Table 4 (continued)

Storm event	Site	Number of samples	Time (min)	Rainfall amount (mm)	TN (mg/L)	DTN	TSS	COD	NH_4^+	NO_3^-
			90	0.03	1.02	0.80	82	86.30	0.07	0.10
			95	0.03	1.53	0.99	174	208.89	0.04	0.16
20,190,625	A	24	0	0.19	2.81	2.46	38	38.60	0.81	5.05
Storm event 3			5	0.19	1.46	1.35	22	11.80	0.44	1.23
			10	0.28	1.29	1.18	92	19.40	0.43	1.15
			15	0.95	0.59	0.54	68	9.80	0.21	0.37
			20	0.47	0.54	0.45	38	8.60	0.22	0.53
			25	0.47	0.57	0.56	34	11.00	0.12	0.14
			30	0.28	0.68	0.64	46	7.40	0.26	0.45
			35	0.47	0.69	0.57	12	9.00	0.20	0.29
			40	0.19	0.56	0.46	18	9.40	0.12	0.22
			45	0.47	0.65	0.60	18	11.80	0.17	0.34
			50	0.28	0.36	0.35	8	11.80	0.19	0.26
			55	0.19	0.36	0.35	5	6.60	0.13	0.21
			60	0.28	0.28	0.26	8	11.80	0.13	0.16
			65	0.47	0.41	0.38	18	9.00	0.13	0.18
			70	0.19	0.41	0.39	46	13.80	0.14	0.19
			75	0.66	0.35	0.34	6	12.20	0.12	0.21
			80	0.66	0.52	0.38	24	22.60	0.12	0.09
			85	0.19	0.27	0.26	46	13.40	0.13	0.18
			90	0.19	0.26	0.25	36	10.60	0.11	0.14
			95	0.19	0.38	0.36	26	13.80	0.13	0.15
			100	0.76	0.33	0.32	46	14.60	0.13	0.18
			105	0.19	0.32	0.20	40	10.60	0.14	0.15
			110	0.66	0.30	0.27	5	11.80	0.22	0.23
			115	0.38	0.35	0.33	50	4.60	0.19	0.18
	B	24	0	0.19	7.87	6.53	576	160.89	2.54	10.69
			5	0.19	3.65	2.67	382	305.33	1.04	7.11
			10	0.28	5.27	4.52	86	104.22	1.28	8.47
			15	0.95	8.78	7.24	74	64.96	1.48	6.28
			20	0.47	3.47	2.87	246	412.88	1.18	4.03
			25	0.47	5.70	5.61	342	152.00	1.28	6.88
			30	0.28	5.51	4.18	322	176.07	1.27	4.43
			35	0.47	3.07	3.04	194	439.81	0.76	4.30
			40	0.19	4.07	3.38	100	263.85	1.45	3.27
			45	0.47	3.34	3.06	178	245.33	1.17	3.69
			50	0.28	3.57	2.81	140	153.11	0.99	2.96
			55	0.19	3.85	2.50	230	238.30	0.83	3.88
			60	0.28	4.42	2.87	228	140.15	0.76	2.87
			65	0.47	2.98	2.62	210	143.11	0.74	2.99
			70	0.19	2.96	1.69	256	152.00	0.61	1.81
			75	0.66	2.99	2.53	88	117.93	0.58	3.65
			80	0.66	4.89	3.77	96	86.81	0.67	3.60
			85	0.19	2.89	2.12	130	201.63	0.56	2.05

Table 4 (continued)

Storm event	Site	Number of samples	Time (min)	Rainfall amount (mm)	TN (mg/L)	DTN	TSS	COD	NH_4^+	NO_3^-
			90	0.19	2.83	1.90	98	111.26	0.65	3.17
			95	0.19	2.20	1.70	130	134.96	0.47	3.22
			100	0.76	2.46	1.79	96	62.00	0.36	3.00
			105	0.19	2.15	1.68	108	57.19	0.40	2.68
			110	0.66	1.99	1.74	128	54.96	0.48	2.73
			115	0.38	2.05	2.00	92	52.37	0.41	3.22
20,190,809	A	24	0	1.51	1.59	1.56	30	51.68	0.77	1.17
Storm event 4			5	1.51	1.03	0.84	112	37.39	0.51	0.83
			10	0.04	0.83	0.69	12	19.54	0.28	0.20
			15	2.26	0.84	0.66	108	18.82	0.46	0.76
			20	5.28	0.77	0.61	58	10.25	0.44	0.21
			25	0.04	0.59	0.53	84	12.39	0.37	0.13
			30	0.75	0.55	0.48	58	14.54	0.32	0.26
			35	0.38	0.47	0.34	34	25.96	0.27	0.29
			40	0.38	0.47	0.46	50	8.11	0.23	0.19
			45	0.15	0.49	0.46	56	10.96	0.21	0.12
			50	0.38	0.55	0.49	32	17.04	0.25	0.17
			55	0.38	0.66	0.58	12	9.18	0.16	0.06
			60	0.30	0.65	0.45	50	10.96	0.25	0.32
			65	0.30	0.45	0.39	30	16.32	0.16	0.13
			70	2.26	0.43	0.36	50	10.61	0.17	0.16
			75	2.26	0.62	0.44	38	21.32	0.13	0.12
			80	0.30	0.31	0.29	56	17.38	0.14	0.06
			85	0.30	0.32	0.31	38	14.18	0.11	0.17
			90	0.15	0.44	0.31	22	7.04	0.11	0.32
			95	0.08	0.34	0.25	18	5.61	0.10	/
			100	0.04	0.70	0.40	30	13.82	0.09	0.14
			105	0.02	0.42	0.30	68	7.75	0.09	0.15
			110	0.02	0.35	0.30	52	13.11	0.10	/
			115	0.02	0.41	0.37	28	11.68	0.20	0.25
	B	24	0	1.51	5.09	3.75	220	138.15	1.11	2.58
			5	1.51	5.09	2.54	284	137.00	0.52	/
			10	0.04	4.65	2.59	104	67.38	0.61	1.68
			15	2.26	4.15	0.66	462	242.00	/	0.29
			20	5.28	3.39	0.99	420	208.15	0.35	0.37
			25	0.04	1.80	0.29	396	159.69	0.02	0.11
			30	0.75	1.53	0.69	366	163.54	0.18	2.25
			35	0.38	2.41	0.65	302	128.54	0.02	0.15
			40	0.38	1.45	0.80	178	73.54	0.13	0.97
			45	0.15	1.88	1.18	250	91.62	0.18	0.86
			50	0.38	1.66	0.99	170	62.38	0.14	1.15
			55	0.38	1.89	1.28	312	77.77	0.23	1.43
			60	0.30	2.12	1.54	126	37.38	0.22	1.21
			65	0.30	2.13	1.63	130	83.54	0.18	1.17

Table 4 (continued)

Storm event	Site	Number of samples	Time (min)	Rainfall amount (mm)	TN (mg/L)	DTN	TSS	COD	NH_4^+	NO_3^-
			70	2.26	2.18	1.52	298	75.08	0.13	1.11
			75	2.26	1.58	0.44	334	160.08	0.01	/
			80	0.30	1.95	1.37	118	68.54	0.25	1.48
			85	0.30	1.89	1.37	136	40.08	0.18	2.09
			90	0.15	1.53	1.37	48	42.00	0.15	1.65
			95	0.08	1.52	0.87	206	100.46	0.21	1.24
			100	0.04	1.78	0.97	288	120.08	0.11	1.28
			105	0.02	1.77	1.51	60	51.62	0.18	1.87
			110	0.02	2.07	1.82	86	43.15	0.15	2.60
			115	0.02	1.98	1.65	57	47.77	0.12	2.67
20,200,515	A	24	0	0.94	1.83	1.77	38	68.08	0.82	2.04
Storm event 5			5	0.05	1.55	1.34	48	47.69	0.48	1.33
			10	0.47	1.35	1.10	78	60.00	0.49	1.05
			15	0.05	0.91	0.88	4	22.69	0.26	0.75
			20	0.47	0.89	0.80	40	23.46	0.29	0.64
			25	0.94	1.22	0.68	40	30.00	0.25	0.36
			30	0.05	0.94	0.57	44	20.77	0.22	0.54
			35	0.19	0.72	0.63	42	17.69	0.14	0.22
			40	0.47	0.63	0.52	22	25.77	0.20	0.34
			45	0.28	0.80	0.61	56	25.77	0.42	0.47
			50	0.38	0.73	0.70	40	34.62	0.11	0.49
			55	0.38	0.58	0.50	32	31.92	0.04	0.29
			60	0.05	0.88	0.64	38	30.00	0.12	0.51
			65	0.09	0.79	0.49	6	15.77	0.10	0.59
			70	0.09	0.94	0.83	54	45.77	0.12	0.56
			75	0.47	0.82	0.54	12	29.23	0.11	0.40
			80	0.47	0.70	0.45	40	32.31	0.07	0.31
			85	0.04	0.66	0.42	2	15.00	0.07	0.38
			90	0.47	0.65	0.42	4	16.92	0.06	0.15
			95	0.02	0.48	0.40	0	11.15	0.11	0.38
			100	0.02	1.09	0.46	0	31.15	0.12	0.52
			105	0.01	1.05	0.89	24	39.62	0.07	0.17
			110	0.01	0.97	0.60	10	43.08	0.16	0.57
			115	0.01	0.87	0.56	20	44.23	0.14	0.51
	B	20	0	0.47	10.21	5.28	978	368.08	1.21	0.07
			5	0.94	8.85	2.05	578	431.54	0.05	/
			10	0.05	7.07	2.29	866	384.23	0.87	0.70
			15	0.19	7.32	1.82	558	430.38	/	/
			20	0.47	3.37	1.24	266	208.85	0.32	0.96
			25	0.28	3.31	1.46	274	150.00	0.65	1.19
			30	0.38	5.10	1.65	670	317.69	0.41	0.82
			35	0.38	5.83	1.80	690	428.08	0.64	0.56
			40	0.05	4.24	1.56	290	214.62	0.50	0.50
			45	0.09	2.79	1.35	204	230.00	0.50	0.50

Table 4 (continued)

Storm event	Site	Number of samples	Time (min)	Rainfall amount (mm)	TN (mg/L)	DTN	TSS	COD	NH_4^+	NO_3^-
			50	0.09	4.28	1.30	324	244.62	0.43	0.44
			55	0.47	2.81	0.99	168	123.85	0.29	0.22
			60	0.47	4.91	2.09	598	306.15	0.79	0.61
			65	0.04	4.65	1.57	258	213.46	0.67	0.66
			70	0.47	4.49	1.18	238	300.77	0.58	0.60
			75	0.02	4.04	1.15	198	238.08	0.34	0.45
			80	0.02	2.46	0.63	56	105.00	0.31	0.53
			85	0.01	3.27	1.05	114	122.31	0.35	0.63
			90	0.01	4.69	1.54	286	424.23	0.51	0.23
			95	0.01	2.18	1.36	52	96.92	0.36	1.38
20,200,616	A	25	0	0.96	3.51	3.33	138	61.24	1.74	4.64
Storm event 6			5	2.55	2.38	1.98	38	13.31	0.88	2.34
			10	2.23	3.74	3.13	12	16.07	2.24	4.36
			15	0.64	3.99	3.87	6	23.31	2.27	4.72
			20	0.03	3.32	3.24	110	62.28	2.04	3.75
			25	0.64	1.89	1.78	62	14.69	0.95	1.66
			30	2.55	0.78	0.54	30	10.90	0.30	0.45
			35	1.28	0.59	0.46	30	7.10	0.25	0.50
			40	0.64	0.86	0.54	2	5.38	0.34	0.71
			45	0.64	1.13	0.71	48	9.17	0.45	1.06
			50	0.03	1.31	0.90	18	17.45	0.50	1.08
			55	0.03	1.55	1.21	60	29.17	0.68	1.66
			60	0.32	1.70	1.43	38	28.14	0.37	0.95
			65	0.51	1.61	1.39	30	38.83	0.64	2.32
			70	0.32	0.73	0.72	26	34.00	0.38	1.16
			75	0.96	0.48	0.36	16	18.14	0.23	0.41
			80	0.06	0.57	0.41	18	16.07	0.27	0.57
			85	0.89	0.33	0.21	12	10.21	0.16	0.35
			90	0.32	0.60	0.41	6	11.59	0.26	0.89
			95	0.06	0.93	0.82	40	31.24	0.51	0.96
			100	0.02	0.98	0.73	10	32.97	0.55	1.34
			105	0.02	1.15	0.95	24	25.03	0.67	1.41
			110	0.57	1.26	0.99	42	34.69	0.48	1.16
			115	0.01	0.76	0.66	2	27.79	0.38	0.87
			120	0.01	0.77	0.75	10	35.72	0.32	0.56
	B	20	0	0.96	4.48	2.76	220	101.59	1.62	/
			5	2.55	3.57	2.04	168	93.66	1.12	0.32
			10	2.23	3.49	2.16	120	100.90	1.55	1.25
			15	0.64	3.72	3.47	92	43.31	1.98	5.42
			20	0.03	3.23	2.67	198	49.86	1.44	3.62
			25	0.64	3.45	1.32	148	48.14	0.83	1.35
			30	2.55	1.86	1.15	90	67.79	0.66	0.71
			35	1.28	1.14	0.84	294	101.93	0.24	1.16
			40	0.64	1.96	1.26	134	49.86	0.46	1.78

Table 4 (continued)

Storm event	Site	Number of samples	Time	Rainfall amount	TN	DTN	TSS	COD	NH_4^+	NO_3^-
			(min)	(mm)	(mg/L)					
			45	0.64	2.02	1.62	154	51.93	0.87	2.01
			50	0.51	2.29	1.82	234	217.79	0.35	1.74
			55	0.32	1.34	0.85	468	186.76	0.23	0.62
			60	0.96	1.16	0.74	484	126.41	0.07	1.13
			65	0.06	1.68	0.90	228	42.62	0.18	0.74
			70	0.89	0.65	0.40	122	87.10	0.02	0.60
			75	0.32	1.16	0.70	320	93.31	0.11	0.70
			80	0.06	0.89	0.59	80	34.69	0.10	0.80
			85	0.02	1.14	0.64	194	69.86	0.17	0.82
			90	0.02	1.40	0.87	130	74.69	0.12	0.47
			95	0.57	0.77	0.56	90	79.86	0.11	0.79
20,200,828	A	23	0	1.23	1.53	1.44	16	11.92	0.93	2.06
Storm event 7			5	0.21	1.09	1.05	16	6.15	0.68	1.07
			10	0.41	1.03	0.92	46	4.62	0.62	1.03
			15	0.82	0.72	0.65	16	4.62	0.45	0.34
			20	0.53	0.96	0.93	18	6.15	0.57	1.07
			25	0.41	1.19	1.07	10	3.46	0.66	0.63
			30	0.08	1.25	1.17	20	18.85	0.76	1.83
			35	0.41	1.05	1.03	12	12.69	0.63	0.96
			40	0.21	1.31	1.19	4	2.69	0.76	1.07
			45	0.04	1.56	1.46	2	4.62	0.80	1.99
			50	0.21	1.52	1.35	6	7.31	0.72	0.87
			55	0.08	1.36	1.27	20	9.23	0.63	1.50
			60	0.04	1.17	1.15	10	7.31	0.56	2.03
			65	0.29	1.09	0.99	12	9.23	0.49	1.29
			70	1.64	1.02	0.95	23	12.31	0.43	1.73
			75	0.21	0.93	0.88	12	6.15	0.44	1.39
			80	0.21	0.93	0.87	8	8.08	0.44	1.64
			85	0.21	0.74	0.70	11	8.46	0.44	1.40
			90	0.21	0.74	0.68	3	2.69	0.46	1.34
			95	0.21	0.71	0.67	2	15.77	0.43	1.36
			100	0.21	0.73	0.66	8	7.31	0.42	1.24
			105	0.12	0.75	0.70	5	9.23	0.44	1.14
			110	0.04	0.93	0.76	10	10.00	0.47	1.23
	B	23	0	1.23	5.67	2.82	254	143.46	0.57	5.67
			5	0.21	6.61	2.68	382	209.23	0.77	6.56
			10	0.41	4.72	2.06	184	116.15	0.63	4.47
			15	0.82	3.45	2.65	164	92.69	0.54	5.79
			20	0.53	4.24	2.28	124	85.00	0.68	4.66
			25	0.41	2.79	2.39	190	72.69	0.77	4.03
			30	0.08	4.48	2.05	154	66.15	0.75	3.15
			35	0.41	2.79	2.15	138	60.00	0.74	3.50
			40	0.21	4.05	1.75	188	210.77	0.77	2.86
			45	0.04	4.06	1.87	444	253.46	0.85	2.18

Table 4 (continued)

Storm event	Site	Number of samples	Time (min)	Rainfall amount (mm)	TN (mg/L)	DTN	TSS	COD	NH_4^+	NO_3^-
			50	0.21	3.16	1.36	182	106.15	0.23	2.58
			55	0.08	3.06	1.47	162	95.77	0.18	2.31
			60	0.04	1.92	1.22	110	53.08	0.15	2.02
			65	0.29	2.39	1.55	64	60.77	0.18	2.36
			70	1.64	1.82	1.12	52	124.62	0.15	1.96
			75	0.21	1.83	1.10	30	29.62	0.25	1.87
			80	0.21	1.47	0.98	62	19.23	0.25	1.16
			85	0.21	1.10	0.71	4	31.54	0.14	0.91
			90	0.21	1.53	1.07	44	8.08	0.21	1.24
			95	0.21	1.23	0.89	48	8.46	0.19	1.48
			100	0.21	1.42	1.38	64	15.00	0.22	1.72
			105	0.12	1.75	1.18	54	21.92	0.23	2.67
			110	0.04	2.20	1.57	76	40.00	0.48	2.19

et al., 2019). The $\delta^{15}N\text{-}NO_3^-$ values in roof and road runoff in the urban residential area in Hangzhou were higher than the $\delta^{15}N\text{-}NO_3^-$ values in forest runoff (mean: -6.07‰) reported by Zhang et al. (2019) because chemical fertilisers with low $\delta^{15}N\text{-}NO_3^-$ values were identified as the main NO_3^- source in forest runoff. The $\delta^{15}N\text{-}NO_3^-$ and $\delta^{18}O\text{-}NO_3^-$ values of roof and road runoff portrayed in Fig. 3 demonstrate that atmospheric deposition was the only NO_3^- source in roof runoff, while NO_3^- sources of road runoff mainly reflected a mixture of atmospheric deposition and chemical fertilisers during the study period. Previous studies have pointed out that chemical fertilisers contributed an average of 16–64% of NO_3^--N in road runoff, and a large proportion of N inputs were from chemical fertilisers application for residential lawns and plants in urban residential areas (Muller et al., 2020; Riha et al., 2014; Yang & Toor, 2017). The estimated annual NPK (nitrogen–phosphorus–potassium) compound fertiliser application (containing NO_3^- fertiliser and NH_4^+ fertiliser) in urban green land was found to be 75–150 kg N/ha (two applications on average) in Hangzhou (Teaching Material Office of the Ministry of Labor & Social Security, 2005). Further research has suggested that NO_3^- derived from chemical fertilisers (NO_3^- and NH_4^+ fertiliser) had typical $\delta^{15}N\text{-}NO_3^-$ values from -6‰ to + 6‰, and the $\delta^{18}O\text{-}NO_3^-$ values in NH_4^+ fertiliser and in NO_3^- fertiliser were from -5.0 to + 15.0‰ and + 17.0 to + 25.0‰, respectively (Bateman & Kelly, 2007; Xue et al., 2009). Therefore, chemical fertilisers were one of the main NO_3^- sources, as the green coverage rate (27%) in the study area was high.

The temporal variations of $\delta^{15}N\text{-}NO_3^-$ values in road runoff in the urban residential area in Hangzhou followed a consistent decreasing trend, whereas the temporal variations of $\delta^{15}N\text{-}NO_3^-$ in roof runoff fluctuated up and down smoothly (Fig. 4). It was implied that NO_3^- sources in road runoff were more varied, which were not only derived from atmospheric deposition but also from chemical fertilisers, soil particles containing N, and organic N sources (pet waste, leaf litter, etc.), in comparison with those in roof runoff. Based on the variations of TN and NO_3^- concentrations and the $\delta^{15}N\text{-}NO_3^-$ and $\delta^{18}O\text{-}NO_3^-$ values in stormwater runoff, the first 10 min of the sampling period of each storm event was assumed to be the initial period of stormwater runoff. There are two possible reasons for the high $\delta^{15}N\text{-}NO_3^-$ values in road runoff in the beginning (initial period of stormwater runoff, i.e. the first 10 min of sampling time). First, the elderly population (over 60 years old), accounting for 41.7% of the study area, led to high per-area rates of pet ownership (HZSB, 2020); therefore, pets such as dogs that were kept by retired persons may have excreted faeces on roads or green land in residential areas. For example, dog waste in one urban area of Minnesota has been found to contribute up to 28% of

Table 5 The isotope values ($\delta^{18}O\text{-}NO_3^-$, $\delta^{15}N\text{-}NO_3^-$, $\delta^{18}O\text{-}H_2O$, $\delta D\text{-}H_2O$) of runoff in a residential catchment of Hangzhou, Zhejiang

Storm event	Site	Number of samples	T (min)	$\delta^{18}O\text{-}NO_3^-$ (‰)	$\delta^{15}N\text{-}NO_3^-$	$\delta^{18}O\text{-}H_2O$	$\delta D\text{-}H_2O$
20,190,625	A	10	0	68.63	-2.41		
Storm event 3			5	66.10	-2.54		
			10	49.14	-2.66		
			20	56.14	-1.14		
			30	58.48	-2.16		
			40	57.24	-2.20		
			50	56.04	0.98		
			60	59.93	-0.28		
			70	49.74	-0.84		
			85	53.82	-0.82		
	B	13	0	37.75	1.44	-4.25	-26.08
			5	50.21	-1.38		
			10	47.57	-0.81	-4.40	-27.12
			15	43.70	-1.13		
			20	25.71	-1.02	-4.48	-26.34
			30	25.00	-1.67	-4.43	-26.36
			40	29.48	-3.24	-4.97	-30.29
			50	21.86	-3.66	-5.56	-34.65
			60	29.36	-3.80	-6.06	-39.58
			70	21.91	-5.73	-6.28	-41.83
			85	25.63	-4.82	-6.46	-43.80
			95	23.69	-6.43	-6.41	-44.26
			110	23.38	-6.11	-5.96	-41.09
20,190,809	A	11	0	53.07	1.40		
Storm event 4			5	46.57	-2.20		
			10	48.85	-2.37		
			15	44.69	-2.02		
			20	39.87	-4.06		
			30	47.47	-3.68		
			40	47.88	-2.65		
			50	45.76	-2.69		
			60	49.12	-3.54		
			70	45.58	-2.39		
			90	42.28	-2.78		
	B	11	0	23.35	8.40		
			5	36.60	-1.12		
			10	21.39	-1.06		
			15	17.60	-1.54		
			20	16.60	-0.13		
			30	15.60	-0.16		
			40	26.83	-2.34		
			50	21.83	-4.84		
			60	22.24	-6.85		
			70	22.70	-5.80		
			90	19.47	-8.43		

Table 5 (continued)

Storm event	Site	Number of samples	T	$\delta^{18}O\text{-}NO_3^-$	$\delta^{15}N\text{-}NO_3^-$	$\delta^{18}O\text{-}H_2O$	$\delta D\text{-}H_2O$
			(min)	(‰)			
20,200,828	A	11	0	73.42	-4.09		
Storm event 7			5	75.47	-10.22		
			10	75.14	-7.08		
			15	73.96	-9.92		
			20	72.29	-5.46		
			30	75.03	-6.57		
			40	74.34	-7.70		
			60	79.38	-7.79		
			75	77.39	-8.07		
			90	79.76	-8.60		
			105	76.09	-10.73		
		11	0	67.42	-0.70	-9.90	-67.75
			5	69.75	-1.81	-10.12	-68.71
			10	70.39	-1.70	-10.17	-69.65
			15	70.66	-2.35	-10.24	-69.51
			20	68.59	-2.09	-10.48	-69.95
			30	67.28	-4.16	-10.54	-71.69
			40	65.39	-2.55	-10.27	-71.07
			60	71.89	-4.82	-9.88	-71.68
			70	74.30	-8.64	-9.56	-71.17
			80	72.86	-6.27	-9.84	-71.36
			95	71.59	-5.99	-10.16	-72.17

TN inputs (Hobbie et al., 2017). Second, the mineralisation of organic matter including leaf litter, flower debris, pollen, and seeds from trees, and other plants on the roadsides was also a NO_3^- source in stormwater runoff. Similarly, the highest $\delta^{15}N\text{-}NO_3^-$ value of the first sample in roof runoff was also ascribed to organic N (bird and rodent droppings) on the roof surface during storm events 4 and 7. After the surface pollutants were washed away, the soil moisture gradually become saturated. Then, nitrified soil and chemical fertilisers were washed into the road runoff as a result of continuous rainstorms. Thus, low $\delta^{15}N\text{-}NO_3^-$ values in road runoff were observed in the middle and late period of stormwater runoff (i.e. after the first 10 min of sampling time). As reported by Baral et al. (2018), the NO_3^- in stormwater runoff during smaller storms mainly originates from atmospheric deposition. In contrast, the NO_3^- contribution from atmospheric deposition may be lower than that from nitrified soil and fertiliser washed into the stormwater runoff during larger storms. Therefore, in this study, atmospheric deposition is thought to be the main NO_3^- source in road runoff of storm event 7 due to the small rainfall amount and relatively short antecedent dry weather period during the sampling period, which was confirmed by the lower $\delta^{15}N\text{-}NO_3^-$ values and higher $\delta^{18}O\text{-}NO_3^-$ values during storm event 7.

The $\delta^{18}O\text{-}NO_3^-$ values are a useful indicator for identifying whether nitrification occurred during runoff. Theoretically, the $\delta^{18}O\text{-}NO_3^-$ of nitrification is generated by one oxygen atom from oxygen in the atmosphere, and two oxygen atoms from water. The equation can be expressed as $\delta^{18}O\text{-}NO_3^- = 2/3\ (\delta^{18}O\text{-}H_2O) + 1/3\ (\delta^{18}O\text{-}O_2)$ (Kendall et al., 2007). According to this equation, the observed $\delta^{18}O_{\text{-H2O}}$ values of water samples and $\delta^{18}O\text{-}O_2$ (+23.5‰), it was expected that the theoretical $\delta^{18}O\text{-}NO_3^-$ values in the road runoff from nitrification could range from +0.8‰ to +5.0‰, which was considerably lower than the obsreved $\delta^{18}O\text{-}NO_3^-$ values in the road runoff in storm events 3 and 7 (Fig. 5). Therefore,

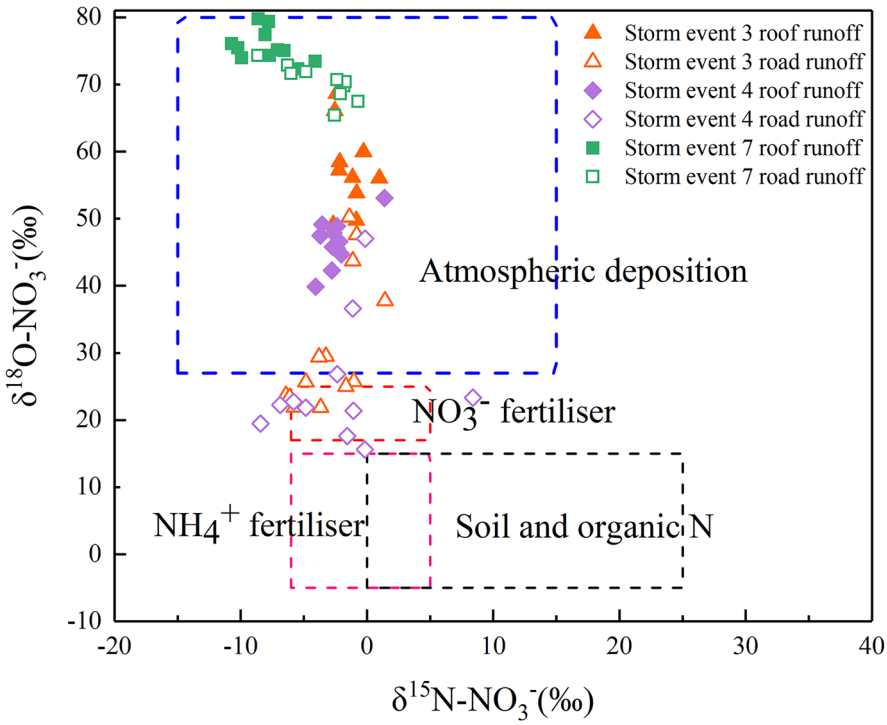

Fig. 3 δ^{15}N-NO_3^- and δ^{18}O-NO_3^- values of stormwater runoff in the urban residential catchment for storm events 3, 4, and 7

the possibility of an instant nitrate production within the runoff water was eliminated. Generally, denitrification occurs when oxygen is limited and organic carbon is available in an aquatic ecosystem, where bacteria reduce NO_3^- to N_2 or N_2O. Heterotrophic microorganisms metabolise light isotopes (i.e. ^{14}N and ^{16}O) in preference to heavy isotopes (i.e. ^{15}N and ^{18}O) during denitrification (Kendall et al., 2007). Denitrification causes the δ^{15}N-NO_3^- and δ^{18}O-NO_3^- values of the residual NO_3^- to increase with a δ^{15}N-NO_3^-/δ^{18}O-NO_3^- ratio from 1:1 to 2:1 (Xue et al., 2009). In this study, no linear relationships between δ^{15}N-NO_3^- and δ^{18}O-NO_3^- were observed, suggesting that no instant denitrification occurred in the roof or road runoff in the urban residential area of Hangzhou.

Estimating the contribution of NO_3^- sources

According to the above analysis, two NO_3^- sources (atmospheric deposition and soil and organic N such as bird and rodent droppings) in roof runoff and four NO_3^- sources (atmospheric deposition, NO_3^- fertiliser, NH_4^+ fertiliser, and soil and organic N such as pet waste, leaf litter and soil N) were identified in road runoff in the urban residential area of Hangzhou. The contributions of NO_3^- in the urban residential stormwater runoff were estimated using the SIAR model. The δ^{15}N-NO_3^- and δ^{18}O-NO_3^- values of the NO_3^- sources were based on relevant literatures (Bedard-Haughn et al., 2003; Curt et al., 2004; Divers et al., 2014; Jin et al., 2019; Kendall et al., 2007; Li et al., 2007b; Widory et al., 2004; Yang & Toor, 2016), as shown in Table 3. We assumed $C_{jk}=0$ in the SIAR model because of the absence of denitrification in the roof and road runoff in the study area. The contributions of NO_3^- sources to roof and road runoff are shown in Fig. 6 and Table S2. The NO_3^- contributions from atmospheric deposition (84–98%) were predominant, and the contributions from organic N were only 2.0–16% in roof runoff. In road runoff, atmospheric deposition (41% in storm event 3; 34% in storm event 4) contributed the most, while soil and organic N (6.0% in storm event 3, 12% in storm event 4) contributed the least, and NH_4^+ fertiliser (31% in storm event 3; 30% in storm event 4), and NO_3^- fertiliser (22% in storm event 3; 24% in storm event 4) were intermediate. The contribution of atmospheric deposition (92%) was dominant, followed by that of NO_3^- fertiliser (3.7%), NH_4^+ fertiliser (2.5%), and

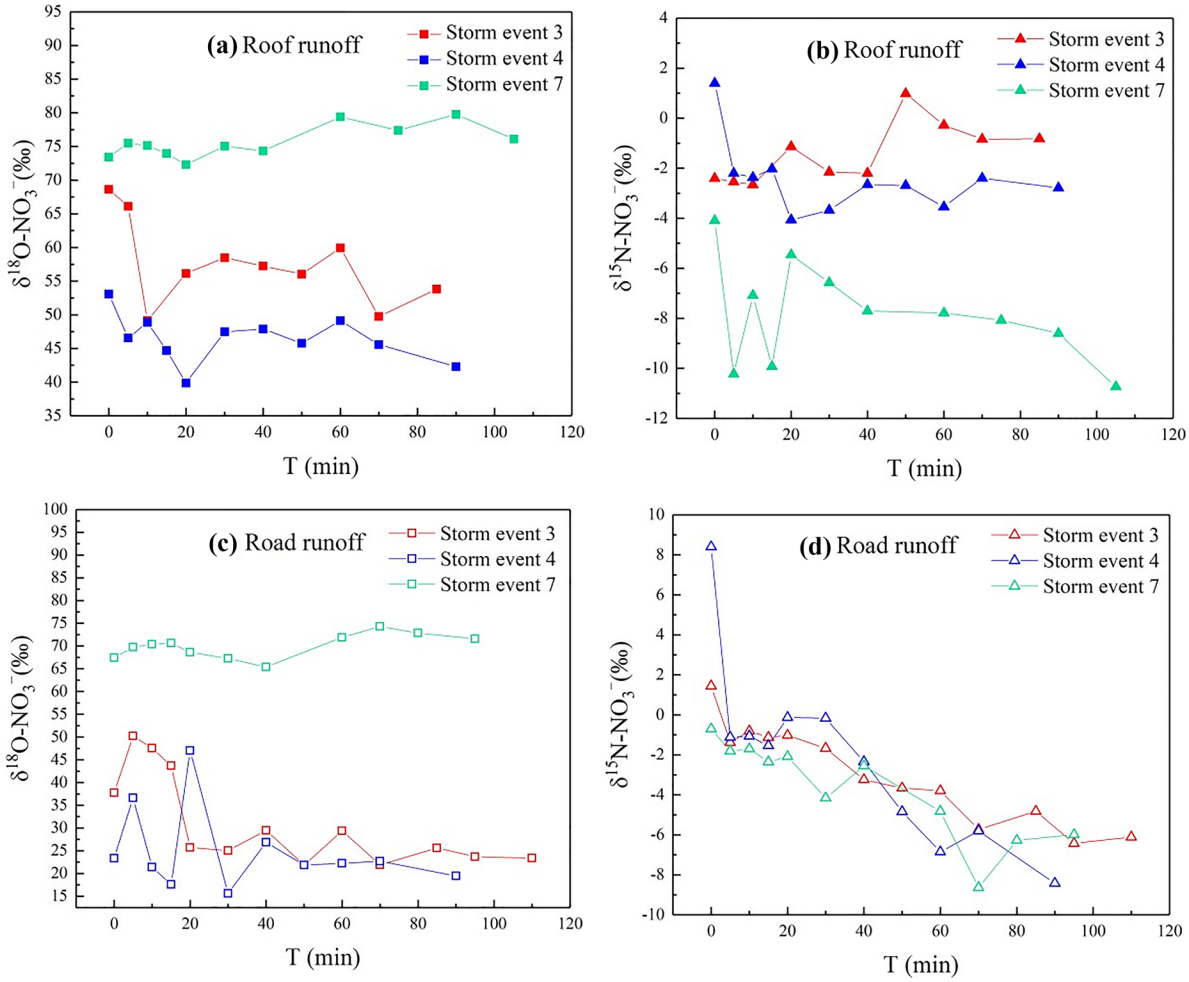

Fig. 4 Temporal variations of $\delta^{15}N\text{-}NO_3^-$ and $\delta^{18}O\text{-}NO_3^-$ in (a)–(b) roof runoff and (c)–(d) road runoff

soil and organic N (1.8%) in road runoff during storm event 7. In this case, atmospheric deposition was an important contributor to stormwater runoff N in the urban residential area, which is similar to the findings of urban stormwater runoff in Florida, where 30–88% of NO_3^- was found to be from atmospheric deposition (Krimsky et al., 2021; Yang & Toor, 2016). Compared with the values in storm events 3 and 4 in this study, a significant increase in the contribution of atmospheric deposition occurred for roof and road runoff during storm event 7, reflecting the short antecedent dry weather period (1 day). Rain from the previous day would have washed away the N pollutants on the road surface. Accordingly, the NO_3^- contributions in road runoff from chemical fertiliser (NH_4^+ fertiliser and NO_3^- fertiliser), and soil and organic N were relatively low for storm event 7. Our results highlighted that chemical fertiliser (NH_4^+ and NO_3^- fertiliser) were the main NO_3^- source in road runoff (an average contribution of more than 50% in road runoff in storm events 3 and 4), owing to the application of chemical fertilisers for plant growth in urban residential areas. This is in agreement with the investigations in urban areas by Hale et al. (2014) and Krimsky et al. (2021). For example, chemical fertilisers contributed 44% of NO_3^- in stormwater runoff in the urban areas of Phoenix, Arizona (Hale et al., 2014). The NO_3^- contribution from soil and organic N was lower than other NO_3^- sources in road runoff in the urban residential area of Hangzhou. Soil erosion was mitigated by 27% of the green land and 73% of the impervious surface, and road sweeping

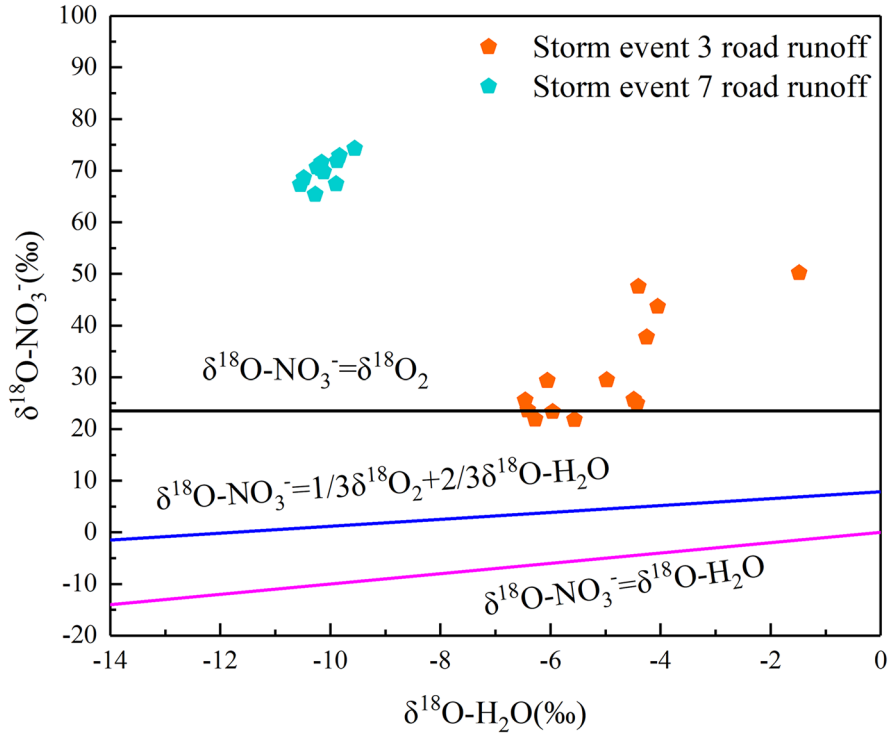

Fig. 5 Relationship between $\delta^{18}O\text{-}H_2O$ and $\delta^{18}O\text{-}NO_3^-$ in the road runoff of storm events 3 and 7

was carried out on alternate days. Although soil and organic N generally have diverse origins, the quantities of soil particles, leaf litter, and pet waste, etc., that were washed into runoff were likely small.

The SIAR outputs revealed that NO_3^- contributions varied significantly between the initial period and middle and late periods in road runoff during a storm event (Fig. 7 and Table S2). The NO_3^- contributions were similar during the same period in storm events 3 and 4. Atmospheric deposition and chemical fertiliser were the primary N sources in both the initial period and middle and late periods in road runoff in storm events 3 and 4. Coupled with the continuing storm, the combination of atmospheric deposition

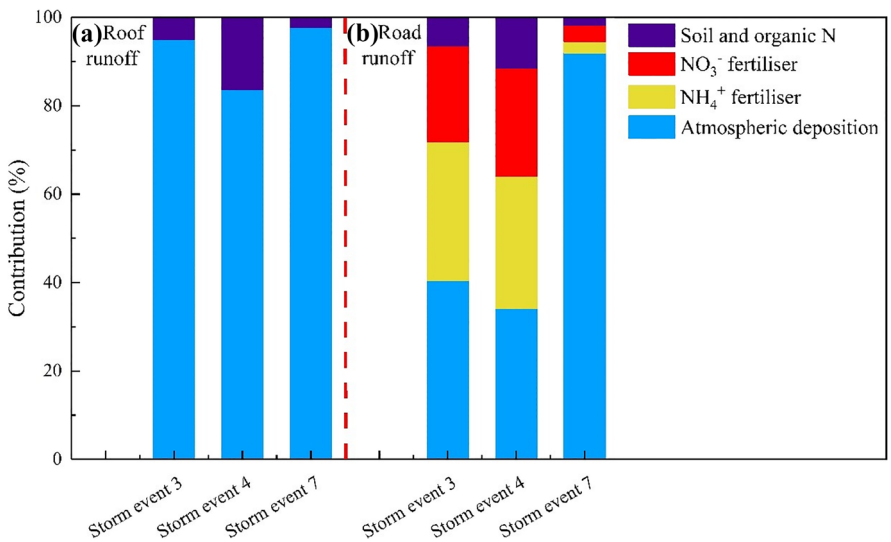

Fig. 6 Contributions of different nitrate sources in roof runoff and road runoff for storm events 3, 4, and 7

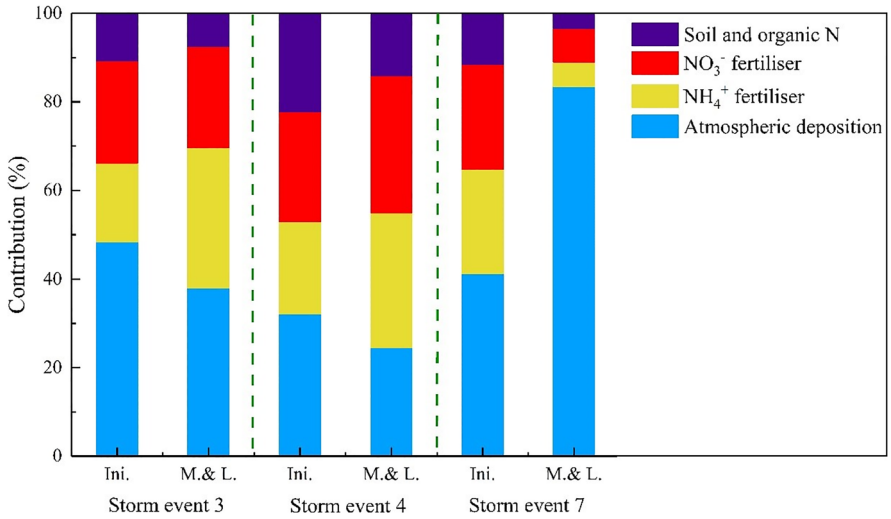

Fig. 7 Contributions of different nitrate sources in road runoff during different periods of the storm events. Ini.: initial period of stormwater runoff (first 10 min of sampling time); M.&L.: middle and late periods of stormwater runoff (after the first 10 min of sampling time)

and chemical fertilisers became more important, suggesting that longer duration storms were more likely to transfer N pollutants from urban green land or urban soils to stormwater runoff. Therefore, we find that during the initial period of stormwater runoff, the storm runoff generated from impervious surfaces was able to quickly wash off the soil, organic matter, and atmospheric dry-deposited NO_3^- on the impervious surface. Thus, the NO_3^- contributions from atmospheric deposition, soil and organic N were higher in the initial period than those in the middle and late periods in road runoff during storm events 3 and 4. Similarly, Lewis and Grimm (2007) revealed that frequent N transport by rain is easier in urban environments. The short antecedent dry weather period (1 day) in storm event 7 was therefore likely responsible for the higher NO_3^- contribution from chemical fertilisers in road runoff during the initial period as compared to the middle and late periods. Moreover, with a decrease in NO_3^- contribution from chemical fertilisers, and soil and organic N, the NO_3^- contribution from atmospheric deposition in road runoff increased dramatically during the middle and late periods for storm event 7.

However, the overlapping in isotope values of NO_3^- sources and the isotopic fractionation effect in N transformation processes might affect the NO_3^- source apportionment by SIAR (Hu et al., 2021; Liu et al., 2018; Yu et al., 2020). In order to reduce the uncertainties and to improve the accuracy of SIAR outputs, the actual values of NO_3^- sources in the study area will be measured and the isotopic fractionation effect in N transformation processes in urban runoff will be considered in the future studies. In addition, it was found that our SIAR outputs about the NO_3^- contributions of the different sources at the different sampling time in the same sampling site have relatively large variations. Therefore, future studies can be paid attention to the temporal variability of NO_3^- isotopes in sampling sites.

Conclusions

The different forms of N and multiple isotopes ($\delta D\text{-}H_2O$, $\delta^{18}O\text{-}H_2O$, $\delta^{15}N\text{-}NO_3^-$, and $\delta^{18}O\text{-}NO_3^-$) in stormwater runoff were measured from 2019 to 2020 in a typical urban residential area in Hangzhou, East China. Based on the findings, N concentrations in road runoff were higher than those in roof runoff. The SIAR model showed that atmospheric deposition was the dominant NO_3^- source, contributing 84–98% of the NO_3^- in roof runoff in 3 storm events. Atmospheric deposition and chemical fertilisers were the major NO_3^- sources in road runoff in 3 storm events, with NO_3^- contributions from atmospheric deposition, NH_4^+-N fertiliser and NO_3^--N fertiliser accounted for 34–92%, 2.5–31%, and 3.7–24%, respectively. The contributions of soil and organic N to NO_3^- in roof and road runoff were relatively low (1.8–16%). The antecedent dry weather period before storm event had a significant impact on NO_3^- in road runoff, and with the increased antecedent dry weather period the NO_3^- contribution of chemical fertilisers was

dramatically increased. It was demonstrated that much of the NO_3^- in road runoff originated from impervious areas (soil and organic N) during the initial period of stormwater runoff. The results of this study suggest that it is necessary to take effective measures to optimise chemical fertilisers application and control its loss from urban green land. Frequent road sweeping and cleaning are useful in preventing soil and organic N from entering urban ecosystems. Reducing the amount of impervious areas is also essential to reducing the overall N load in urban ecosystems.

Acknowledgements The authors gratefully acknowledge the financial support from the National Natural Science Foundation of China (No. 41673097; No. 41977150; No. 41373122).

Author's contributions **Qiyue Hu** contributed to methodology, software, validation, formal analysis, investigation, data curation, writing—original draft, writing—review and editing, and visualization. **Song Zhu** contributed to investigation, software, and resources. **Zanfang Jin** contributed to conceptualization, methodology, software, validation, investigation, resources, data curation, writing—review and editing, supervision, project administration, and funding acquisition. **Aijing Wu** contributed to investigation, data curation, and visualization. **Xiaoyu Chen** contributed to investigation. **Feili Li** contributed to resources.

Funding This study was supported by the National Natural Science Foundation of China (No. 41673097; No. 41977150; No. 41373122).

Availability of data and material The datasets analysed during the study are available in the Supplementary Material.

Declarations

Ethics approval Not applicable.

Consent to participate Not applicable.

Consent for publication Not applicable.

Competing interests The authors declare that they have no competing interests.

References

Al Mamoon, A., Jahan, S., He, X., Joergensen, N. E., & Rahman, A. (2019). First flush analysis using a rainfall simulator on a micro catchment in an arid climate. *Science Of the Total Environment, 693*, Article 133552. https://doi.org/10.1016/j.scitotenv.2019.07.358

Ballo, S., Liu, M., Hou, L. J., & Chang, J. (2009). Pollutants in stormwater runoff in Shanghai (China): Implications for management of urban runoff pollution. *Progress in Natural Science-Materials International, 19*(7), 873–880. https://doi.org/10.1016/j.pnsc.2008.07.021

Baral, D., Fisher, J. R., Florek, M. J., Dvorak, B. I., Snow, D. D., & Admiraal, D. M. (2018). Atmospheric contributions of nitrate to stormwater runoff from two urban watersheds. *Journal Of Environmental Engineering, 144*(2), 05017009, Article 05017009. https://doi.org/10.1061/(asce)ee.1943-7870.0001323

Bateman, A., & Kelly, S. (2007). Fertilizer nitrogen isotope signatures. *Isotopes in Environmental and Health Studies, 43*, 237–247. https://doi.org/10.1080/10256010701550732

Bedard-Haughn, A., van Groenigen, J. W., & van Kessel, C. (2003). Tracing 15N through landscapes: potential uses and precautions. *Journal of Hydrology, 272*(1), 175–190. https://doi.org/10.1016/S0022-1694(02)00263-9

Carey, R. O., Hochmuth, G. J., Martinez, C. J., Boyer, T. H., Dukes, M. D., Toor, G. S., & Cisar, J. L. (2013). Evaluating nutrient impacts in urban watersheds: Challenges and research opportunities. *Environmental Pollution, 173*, 138–149. https://doi.org/10.1016/j.envpol.2012.10.004

Chen, X., Jiang, L., Huang, X. L., & Cai, Z. C., (2021). Identifying nitrogen source and transport characteristics of the urban estuaries and gate-controlled rivers in northern Taihu Lake, China. *Ecological Indicators*, *130*, Article 108035. https://doi.org/10.1016/j.ecolind.2021.108035

Chong, N.-M., Chen, Y.-C., & Hsieh, C.-N. (2012). Assessment of the quality of stormwater from an industrial park in central Taiwan. *Environmental Monitoring and Assessment, 184*(4), 1801–1811. https://doi.org/10.1007/s10661-011-2079-6

Chow, M. F., & Yusop, Z. (2014). Characterization and source identification of stormwater runoff in tropical urban catchments. *Water Science and Technology, 69*(2), 244–252. https://doi.org/10.2166/wst.2013.574

Craig, H. I. (1961). Isotopic variations in meteoric waters: Science. *Science, 133*.

Curt, M., Aguado, P. L., Sánchez, G., Bigeriego, M., & Fernández, J. (2004). Nitrogen isotope ratios of synthetic and organic sources of nitrate water contamination in Spain. *Water Air and Soil Pollution, 151*, 135–142. https://doi.org/10.1023/B:WATE.0000009889.36833.c0

Divers, M. T., Elliott, E. M., & Bain, D. J. (2014). Quantification of Nitrate Sources to an Urban Stream Using Dual Nitrate Isotopes. *Environmental Science & Technology, 48*(18), 10580–10587. https://doi.org/10.1021/es404880j

Dong, Y., Yang, J. L., Zhao, X. R., Yang, S. H., Jan Mulder, J., Dörsch, P., & Zhang, G. L. (2021). Nitrate runoff loss and source apportionment in a typical subtropical agricultural watershed. *Environmental Science and Pollution Research*. https://doi.org/10.1007/s11356-021-16935-3

Gómez-Alday, J. J., Hussein, S., Arman, H., Alshamsi, D., Murad, A., Elhaj, K., & Aldahan, A. (2022). A multi-isotopic evaluation of groundwater in a rapidly developing area and implications for water management in hyper-arid regions. *Science of the Total Environment*, *805*, Article 150245. https://doi.org/10.1016/j.scitotenv.2021.150245

Gromaire-Mertz, M. C., Garnaud, S., Gonzalez, A., & Chebbo, G. (1999). Characterisation of urban runoff pollution in Paris. *Water Science and Technology, 39*(2), 1–8. https://doi.org/10.1016/s0273-1223(99)00002-5

Hale, R. L., Turnbull, L., Earl, S., Grimm, N., Riha, K., Michalski, G., Lohse, K. A., & Childers, D. (2014). Sources and Transport of Nitrogen in Arid Urban Watersheds. *Environmental Science & Technology, 48*(11), 6211–6219. https://doi.org/10.1021/es501039t

Hobbie, S. E., Finlay, J. C., Janke, B. D., Nidzgorski, D. A., Millet, D. B., & Baker, L. A. (2017). Contrasting nitrogen and phosphorus budgets in urban watersheds and implications for managing urban water pollution (vol 114, pg 4177, 2017). *Proceedings of the National Academy of Sciences of the United States of America, 114*(20), E4116–E4116. https://doi.org/10.1073/pnas.1706049114

Hu, J., Pan, M. Y., Han, T. H., Zhuang, Z., Cao, Y. N., Yang, K. L., Li, Y. L., & Liu, W. G. (2021). Identification of nitrate sources in the Jing River using dual stable isotopes, Northwest China. *Environmental Science and Pollution Research.* https://doi.org/10.1007/s11356-021-15380-6

Hu, M. P., Liu, Y. M., Zhang, Y. F., Dahlgren, R. A., & Chen, D. J. (2019). Coupling stable isotopes and water chemistry to assess the role of hydrological and biogeochemical processes on riverine nitrogen sources. *Water Research, 150*, 418–430. https://doi.org/10.1016/j.watres.2018.11.082

HZSB. (2020). Hangzhou Bureau of Statistics, 2020. Hangzhou Statistical Yearbook. https://tjj.hangzhou.gov.cn/art/2020/10/29/art_1229453592_3819709.html. Accessed 29 October 2020.

Jani, J., Yang, Y. Y., Lusk, M. G., & Toor, G. S. (2020). Composition of nitrogen in urban residential stormwater runoff: Concentrations, loads, and source characterization of nitrate and organic nitrogen. *Plos One, 15*(2), e0229715, Article e0229715. https://doi.org/10.1371/journal.pone.0229715

Janke, B. D., Finlay, J. C., & Hobbie, S. E. (2017). Trees and Streets as Drivers of Urban Stormwater Nutrient Pollution. *Environmental Science & Technology, 51*(17), 9569–9579. https://doi.org/10.1021/acs.est.7b02225

Jin, Z. F., Hu, J., Wu, A. J., Li, G. Y., Zhang, W. L., & Li, F. L. (2021a). Identify the Nitrate Sources in Different Land Use Areas Based on Multiple Isotopes. *Environmental Science, 42*(4), 1696–1705. (In Chinese).

Jin, Z. F., Qian, L. J., Shi, Y. S., Fu, G. W., Li, G. Y., & Li, F. L. (2021b). Quantifying major NOx sources of aerosol nitrate in Hangzhou, China, by using stable isotopes and a Bayesian isotope mixing model. *Atmospheric Environment, 244*, 117979, Article 117979. https://doi.org/10.1016/j.atmosenv.2020.117979

Jin, Z. F., Wang, Y., Qian, L. J., Hu, Y. M., Jin, X. P., Hong, C. C., & Li, F. L. (2019). Combining chemical components with stable isotopes to determine nitrate sources of precipitation in Hangzhou and Huzhou, SE China. *Atmospheric Pollution Research, 10*(2), 386–394. https://doi.org/10.1016/j.apr.2018.09.004

Kaiser, J., Hastings, M. G., Houlton, B. Z., Rockmann, T., & Sigman, D. M. (2007). Triple oxygen isotope analysis of nitrate using the denitrifier method and thermal decomposition of N2O. *Analytical Chemistry, 79*(2), 599–607. https://doi.org/10.1021/ac061022s

Kaushal, S. S., Mayer, P. M., Vidon, P. G., Smith, R. M., Pennino, M. J., Newcomer, T. A., Duan, S. W., Welty, C., & Belt, K. T. (2014). Land use and climate variability amplify carbon, nutrient, and contaminant pulses: A review with management implications. *Journal of the American Water Resources Association, 50*(3), 585–614. https://doi.org/10.1111/jawr.12204

Kendall, C., Elliott, E., & Wankel, S. (2007). Tracing Anthropogenic Inputs of Nitrogen to Ecosystems. In (pp. 375–449). https://doi.org/10.1002/9780470691854.ch12

Kim, L. H., Ko, S. O., Jeong, S., & Yoon, J. (2007). Characteristics of washed-off pollutants and dynamic EMCs in parking lots and bridges during a storm. *Science of the Total Environment, 376*(1–3), 178–184. https://doi.org/10.1016/j.scitotenv.2006.12.053

Kojima, K., Murakami, M., Yoshimizu, C., Tayasu, I., Nagata, T., & Furumai, H. (2011). Evaluation of surface runoff and road dust as sources of nitrogen using nitrate isotopic composition. *Chemosphere, 84*(11), 1716–1722. https://doi.org/10.1016/j.chemosphere.2011.04.071

Krimsky, L. S., Lusk, M. G., Abeels, H., & Seals, L. (2021). Sources and concentrations of nutrients in surface runoff from waterfront homes with different landscape practices. *Science Of the Total Environment, 750*, 142320, Article 142320. https://doi.org/10.1016/j.scitotenv.2020.142320

Lee, J. H., Bang, K. W., Ketchum, L. H., Choe, J. S., & Yu, M. J. (2002). First flush analysis of urban storm runoff. *Science Of the Total Environment, 293*(1–3), 163–175, Article Pii s0048–9697(02)00006–2. https://doi.org/10.1016/s0048-9697(02)00006-2

Lewis, D. B., & Grimm, N. B. (2007). Hierarchical regulation of nitrogen export from urban catchments: Interactions of storms and landscapes. *Ecological Applications, 17*(8), 2347–2364. https://doi.org/10.1890/06-0031.1

Li, D. Y., Wan, J. Q., Ma, Y. W., Wang, Y., Huang, M. Z., & Chen, Y. M. (2015). Stormwater Runoff Pollutant Loading Distributions and Their Correlation with Rainfall and Catchment Characteristics in a Rapidly Industrialized City. *Plos One, 10*(3), e0118776, Article e0118776. https://doi.org/10.1371/journal.pone.0118776

Li, L. Q., Yin, C. Q., He, Q. C., & Kong, L. L. (2007a). First flush of storm runoff pollution from an urban catchment in China. *Journal of Environmental Sciences, 19*(3), 295–299. https://doi.org/10.1016/s1001-0742(07)60048-5

Li, M. T., Chen, J., Finlayson, B., Chen, Z. Y., Webber, M., Barnett, J., & Wang, M. (2019a). Freshwater Supply to Metropolitan Shanghai: Issues of Quality from Source to Consumers. *Water, 11*(10), 2176, Article 2176. https://doi.org/10.3390/w11102176

Li, Q., Yu, Y., Jiang, X. Q., & Guan, Y. T. (2019b). Multifactor-based environmental risk assessment for sustainable land-use planning in Shenzhen, China. *Science of the Total Environment, 657*, 1051–1063. https://doi.org/10.1016/j.scitotenv.2018.12.118

Li, X., Masuda, H., Koba, K., & Zeng, H. (2007b). Nitrogen Isotope Study on Nitrate-Contaminated Groundwater in the Sichuan Basin, China. *Water, Air, and Soil Pollution, 178*, 145–156. https://doi.org/10.1007/s11270-006-9186-y

Liu, M., Seyf-Laye, A.-S.M., Ibrahim, T., Gbandi, D.-B., & Chen, H. (2014). Tracking sources of groundwater

nitrate contamination using nitrogen and oxygen stable isotopes at Beijing area, China. *Environmental Earth Sciences, 72*(3), 707–715. https://doi.org/10.1007/s12665-013-2994-7

Liu, S. S., Wu, F. C., Feng, W. Y., Guo, W. J., Song, F. H., Wang, H., Wang, Y., He, Z. Q., Giesy, J. P., Zhu, P., & Tang, Z. (2018). Using dual isotopes and a Bayesian isotope mixing model to evaluate sources of nitrate of Tai Lake, China. *Environmental Science and Pollution Research, 25*, 32631–32639. https://doi.org/10.1007/s11356-018-3242-1

Liu, X. L., Han, G. L., Zeng, J., Liu, M., Li, X. Q., & Boeckx, P. (2021). Identifying the sources of nitrate contamination using a combined dual isotope, chemical and Bayesian model approach in a tropical agricultural river: Case study in the Mun River, Thailand. *Science Of the Total Environment, 760*, 143938, Article 143938. https://doi.org/10.1016/j.scitotenv.2020.143938

Lusk, M. G., & Toor, G. S. (2016). Biodegradability and Molecular Composition of Dissolved Organic Nitrogen in Urban Stormwater Runoff and Outflow Water from a Stormwater Retention Pond. *Environmental Science & Technology, 50*(7), 3391–3398. https://doi.org/10.1021/acs.est.5b05714

Ma, G., Wang, Y., Bao, X., Hu, Y., Liu, Y., He, L., Wang, T., & Meng, F. (2015). Nitrogen pollution characteristics and source analysis using the stable isotope tracing method in Ashi River, northeast China. *Environmental Earth Sciences, 73*(8), 4831–4839. https://doi.org/10.1007/s12665-014-3786-4

Margalef-Marti, R., Llovet, A., Carrey, R., Ribas, A., Domene, X., Mattana, S., Chin-Pampillo, J., Mondini, C., Alcaniz, J.M., Soler, A., & Otero N., (2021). Impact of fertilization with pig slurry on the isotopic composition of nitrate retained in soil and leached to groundwater in agricultural areas. *Applied Geochemistry, 125*, Article 104832. https://doi.org/10.1016/j.apgeochem.2020.104832

McIlvin, M. R., & Casciotti, K. L. (2011). Technical Updates to the Bacterial Method for Nitrate Isotopic Analyses. *Analytical Chemistry, 83*(5), 1850–1856. https://doi.org/10.1021/ac1028984

Ministry of Ecology and Environment of the PRC. (1990). Water quality–Determination of suspended substance–Gravimetric method (GB11901-1989). The People's Republic of China National Standards. (in Chinese).

Ministry of Ecology and Environment of the PRC. (2007). Water quality–Determination of the chemical oxygen demand–Fast digestion-spectrophotometric method (HJ/T399-2007). The People's Republic of China National Standards on environmental prote. (in Chinese).

Ministry of Ecology and Environment of the PRC. (2012). Water quality-Determination of total nitrogen-Alkaline potassium persulfate digestion UV spectrophotometric method (HJ636-2012). The People's Republic of China National Standards on environmental prote. (in Chinese).

Muller, A., Osterlund, H., Marsalek, J., & Viklander, M. (2020). The pollution conveyed by urban runoff: A review of sources. *Science Of the Total Environment, 709*, 136125, Article 136125. https://doi.org/10.1016/j.scitotenv.2019.136125

Myers, C., Athayde, D., & riscoll, E. D. (1982). EPA's Nationwide Urban Runoff Program Designed to Produce Useful Results. *Civil Engineering—asce, 52*(2), 54–55.

National Meteorological Centre (NMC), (2019). Super Typhoon Lekima. (In Chinese). http://www.cma.gov.cn/2011xwzx/2011xqxxw/2011xzytq/201908/t20190814_533010.html

Parnell, A. C., Inger, R., Bearhop, S., & Jackson, A. L. (2010). Source Partitioning Using Stable Isotopes: Coping with Too Much Variation. *Plos One, 5*(3), e9672, Article e9672. https://doi.org/10.1371/journal.pone.0009672

Pastén-Zapata, E., Ledesma-Ruiz, R., Harter, T., Ramírez, A. I., & Mahlknecht, J. (2014). Assessment of sources and fate of nitrate in shallow groundwater of an agricultural area by using a multi-tracer approach. *Science of the Total Environment, 470–471*, 855–864. https://doi.org/10.1016/j.scitotenv.2013.10.043

Peng, T.-R., Lin, H.-J., Wang, C.-H., Liu, T.-S., & Kao, S.-J. (2012). Pollution and variation of stream nitrate in a protected high-mountain watershed of Central Taiwan: Evidence from nitrate concentration and nitrogen and oxygen isotope compositions. *Environmental Monitoring and Assessment, 184*(8), 4985–4998. https://doi.org/10.1007/s10661-011-2314-1

Rahal, O., Gouaidia, L., Fidelibus, M. D., Marchina, C., Natali, C., & Bianchini, G. (2021). Hydrogeological and geochemical characterization of groundwater in the F'Kirina plain (eastern Algeria). *Applied Geochemistry, 130*, Article 104983. https://doi.org/10.1016/j.apgeochem.2021.104983

Riha, K. M., Michalski, G., Gallo, E. L., Lohse, K. A., Brooks, P. D., & Meixner, T. (2014). High Atmospheric Nitrate Inputs and Nitrogen Turnover in Semi-arid Urban Catchments. *Ecosystems, 17*(8), 1309–1325. https://doi.org/10.1007/s10021-014-9797-x

Silva, C. D., & da Silva, G. B. L. (2020). Cumulative effect of the disconnection of impervious areas within residential lots on runoff generation and temporal patterns in a small urban area. *Journal Of Environmental Management, 253*, 109719, Article 109719. https://doi.org/10.1016/j.jenvman.2019.109719

Silva, T. F. G., Vincon-Leite, B., Lemaire, B. J., Petrucci, G., Giani, A., Figueredo, C. C., & Nascimento, N. D. (2019). Impact of Urban Stormwater Runoff on Cyanobacteria Dynamics in A Tropical Urban Lake. *Water, 11*(5), 946, Article 946. https://doi.org/10.3390/w11050946

Song, Y. L., Du, X. Q., & Ye, X. Y. (2019). Analysis of Potential Risks Associated with Urban Stormwater Quality for Managed Aquifer Recharge. *International Journal Of Environmental Research And Public Health, 16*(17), 3121, Article 3121. https://doi.org/10.3390/ijerph16173121

Sui, Y. Y., Ou, Y., Yan, B. X., Rousseau, A. N., Fang, Y. T., Geng, R. Z., Wang, L. X., & Ye, N. (2020). A dual isotopic framework for identifying nitrate sources in surface runoff in a small agricultural watershed, northeast China. *Journal of Cleaner Production, 246*, 119074, Article 119074. https://doi.org/10.1016/j.jclepro.2019.119074

Taebi, A., & Droste, R. L. (2004). First flush pollution load of urban stormwater runoff. *Journal of Environmental Engineering and Science, 3*(4), 301–309. https://doi.org/10.1139/s04-018

Taylor, G. D., Fletcher, T. D., Wong, T. H. F., Breen, P. F., & Duncan, H. P. (2005). Nitrogen composition in urban runoff - implications for stormwater management. *Water Research, 39*(10), 1982–1989. https://doi.org/10.1016/j.watres.2005.03.022

Teaching Material Office of the Ministry of Labor and Social Security. (2005). *Garden green space maintenance*. China Labor and Social Security Publisher.

Toor, G. S., Occhipinti, M. L., Yang, Y. Y., Majcherek, T., Haver, D., & Oki, L. (2017). Managing urban runoff in residential neighborhoods: Nitrogen and phosphorus in lawn irrigation driven runoff. *Plos One, 12*(6), e0179151, Article e0179151. https://doi.org/10.1371/journal.pone.0179151

Vaze, J., & Chiew, F. H. S. (2004). Nutrient loads associated with different sediment sizes in urban stormwater and surface pollutants. *Journal of Environmental Engineering-Asce, 130*(4), 391–396. https://doi.org/10.1061/(asce)0733-9372(2004)130:4(391)

Wang, S., Feng, X. J., Wang, Y. D., Zheng, Z. C., Li, T. X., He, S. Q., Zhang, X. Z., Yu, H. Y., Huang, H. G., Liu, T., Memon, S. U. R., & Lin, C. W. (2019). Characteristics of nitrogen loss in sloping farmland with purple soil in southwestern China during maize (Zea mays L.) growth stages. *Catena, 182*, 104169, Article Unsp 104169. https://doi.org/10.1016/j.catena.2019.104169

Weitzman, J. N., Brooks, J. R., Mayer, P. M., Rugh, W. D., & Compton, J. E. (2021). Coupling the dual isotopes of water (delta H-2 and delta O-18) and nitrate (delta N-15 and delta O-18): a new framework for classifying current and legacy groundwater pollution. *Environmental Research Letters, 16*(4), Article 045008. https://doi.org/10.1088/1748-9326/abdcef

Wen, H. Z., Xiao, Y., Wang, X. R., & Chu, L. H. (2019). Land-Transfer Events' Effects on the Housing Market: Empirical Evidence from Hangzhou, China. *Journal Of Urban Planning And Development, 145*(2), 04019003, Article 04019003. https://doi.org/10.1061/(asce)up.1943-5444.0000505

Widory, D., Kloppmann, W., Chéry, L., Bonnin, J., Rochdi, H., & Guinamant, J.-L. (2004). Nitrate in Groundwater: An Isotopic Multi-Tracer Approach. *Journal of Contaminant Hydrology, 72*, 165–188. https://doi.org/10.1016/j.jconhyd.2003.10.010

Xue, D., Botte, J., De Baets, B., Accoe, F., & Oertel née Nestler, A., Taylor, P., Cleemput, O., Berglund, M., & Boeckx, P. (2009). Present Limitations and Future Prospects of Stable Isotope Methods for Nitrate Source Identification in Surface and Groundwater. *Water Research, 43*, 1159–1170. https://doi.org/10.1016/j.watres.2008.12.048

Yan, R. H., Li, L. L., & Gao, J. F. (2019). Framework for quantifying rural NPS pollution of a humid lowland catchment in Taihu Basin, Eastern China. *Science of the Total Environment, 688*, 983–993. https://doi.org/10.1016/j.scitotenv.2019.06.114

Yang, H., Zhao, Y., Wang, J. H., Xiao, W. H., Jarsjo, J., Huang, Y., Liu, Y., Wu, J. P., & Wang, H. J. (2020). Urban closed lakes: Nutrient sources, assimilative capacity and pollutant reduction under different precipitation frequencies. *Science Of the Total Environment, 700*, 134531, Article Unsp 134531. https://doi.org/10.1016/j.scitotenv.2019.134531

Yang, Y.-Y., & Toor, G. (2017). Sources and mechanisms of nitrate and orthophosphate transport in urban stormwater runoff from residential catchments. *Water Research, 112*, 176–184. https://doi.org/10.1016/j.watres.2017.01.039

Yang, Y. Y., & Lusk, M. G. (2018). Nutrients in urban stormwater runoff: Current state of the science and potential mitigation options. *Current Pollution Reports, 4*(2), 112–127. https://doi.org/10.1007/s40726-018-0087-7

Yang, Y. Y., & Toor, G. S. (2016). $\delta^{15}N$ and $\delta^{18}O$ reveal the sources of nitrate-nitrogen in urban residential stormwater runoff. *Environmental Science & Technology, 50*(6), 2881–2889. https://doi.org/10.1021/acs.est.5b05353

Yu, L., Zheng, T. Y., Zheng, X. L., Hao, Y. J., & Yuan, R. Y. (2020). Nitrate source apportionment in groundwater using Bayesian isotope mixing model based on nitrogen isotope fractionation. *Science of the Total Environment*, 718, Article 137242. https://doi.org/10.1016/j.scitotenv.2020.137242

Yuan, J., Zhao, B., & Zhang, Q. (2019). Transformation and source identification of N in the upper reaches of the Han River basin, China: evaluated by a stable isotope approach. *Environmental Monitoring and Assessment, 191*(7), Article 475. https://doi.org/10.1007/s10661-019-7603-0

Yue, F. J., Li, S. L., Waldron, S., Wang, Z. J., Oliver, D. M., Chen, X., & Liu, C. Q. (2020). Rainfall and conduit drainage combine to accelerate nitrate loss from a karst agroecosystem: Insights from stable isotope tracing and high-frequency nitrate sensing. *Water Research, 186*, 116388, Article 116388. https://doi.org/10.1016/j.watres.2020.116388

Zhang, H., Kang, X., Wang, X., Zhang, J., & Chen, G. (2019). Quantitative identification of nitrate sources in the surface runoff of three dominant forest types in subtropical China based on Bayesian model. *Science of the Total Environment, 703*, 135074. https://doi.org/10.1016/j.scitotenv.2019.135074

Zhi, X. S., Chen, L., & Shen, Z. Y. (2018). Impacts of urbanization on regional nonpoint source pollution: Case study for Beijing, China. *Environmental Science and Pollution Research, 25*(10), 9849–9860. https://doi.org/10.1007/s11356-017-1153-1.